

# Interaction of multiple ice streams on the Malin Shelf during deglaciation of the last British–Irish Ice Sheet

KIERAN F. CRAVEN,<sup>1,2\*</sup>  STEPHEN MCCARRON,<sup>1</sup>  XAVIER MONTEYS<sup>2</sup> and DAYTON DOVE<sup>3</sup>

<sup>1</sup>Maynooth University Department of Geography, Maynooth, Co Kildare, W23 HW31, Ireland

<sup>2</sup>Geological Survey Ireland, Beggars Bush, Dublin, D04 K7X4, Ireland

<sup>3</sup>British Geological Survey, The Lyell Centre, Research Avenue South, Edinburgh, EH14 4AP, UK

Received 27 September 2019; Revised 19 November 2020; Accepted 27 November 2020

**ABSTRACT:** The Malin Shelf, off north-west Ireland, was an important zone of confluence for marine-based ice streams of the former British–Irish Ice Sheet (BIIS). Legacy geophysical datasets are used to construct models of the seismic character, relative age and distribution of shelf sediments and landforms. Buried and surface landform assemblages provide evidence that during deglaciation of the Late Devensian BIIS, the region was occupied not by a single Hebrides Ice Stream as previously proposed, but by four discrete ice streams, here referred to as the Sea of the Hebrides (SHIS), Inner Hebrides, North Channel and Tory Island ice streams. Our observations of stratigraphic relationships between the deposits of these ice streams indicate physical interactions between them during shelf deglaciation. We interpret an initial dominant cross-shelf flow along the SHIS impeding cross-shelf ice flow from other ice sheet sectors. Following withdrawal of the SHIS grounding line from the shelf edge to mid-shelf bathymetric highs during deglaciation, a reconfiguration of ice sheet flow paths allowed the expansion of smaller cross-shelf ice streams draining central Scotland and north-western Ireland. This internal dynamic behaviour provides a possible physical analogue for time-transgressive flow patterns reported for outlets draining the West Antarctic Ice Sheet.

© 2021 John Wiley & Sons, Ltd.

## Introduction

The palaeoglaciology of former marine-based ice sheets is recorded in the pattern and timing of buried and seabed glacial to deglacial landform and sediment assemblages on shallow, formerly glaciated marine shelves. Reconstructing the behaviour of marine-influenced ice sheets is important to understand the dynamic response of large ice masses to both internal and external forcing, including glaciological, climatic and sea-level variations. The Late Devensian British–Irish Ice Sheet (BIIS) is an example of a partially marine-based ice sheet, the deglacial history of which offers a data-rich analogue for the response of modern marine-terminating ice sheets such as the Greenland or West Antarctica Ice Sheets (Clark *et al.*, 2012). Having well-constrained and detailed palaeoglacial analogues remains important, given our limited understanding of retreat processes for these contemporary ice sheets (Patton *et al.*, 2015).

During the Late Devensian (c. 32–20 ka), the Malin Shelf, north of Ireland and west of Scotland, was an important marine-terminating zone of confluence for BIIS ice from these Scottish and Irish sources (Dunlop *et al.*, 2010; Clark *et al.*, 2012; Howe *et al.*, 2012; Dove *et al.*, 2015; Small *et al.*, 2017; Callard *et al.*, 2018). From ~32 ka, the BIIS developed mainly over Scottish uplands (Brown *et al.*, 2007), with smaller ice dispersal centres in Skye, Mull, Arran, North-Central Ireland and Donegal (Bradwell *et al.*, 2008; Hubbard *et al.*, 2009). Ice extending onto the Malin Shelf drained the NW Sector of the BIIS, with other northern sectors draining to the Hebridean Shelf, the West Shetland Shelf and the North Sea (Bradwell *et al.*, 2008; Dunlop *et al.*, 2010; Clark *et al.*, 2012, 2018; Ó Cofaigh *et al.*, 2012). The Plio-Pleistocene Barra–Donegal Fan complex (BDF), located

along the shelf edge (Fig. 1a) is primary evidence of a large cross-shelf glacial sediment transport system (Armishaw *et al.*, 2000) that has been termed the ‘Hebrides Ice Stream’ (HIS) (Howe *et al.*, 2012) (also referred to as the ‘Barra Fan Ice Stream’; e.g. Callard *et al.*, 2018). The HIS is interpreted to have drained approximately 5–10% of the last BIIS (Dove *et al.*, 2015). The BDF has been shown to contain a rich stratigraphic record of Late Devensian and older glaciations (Armishaw *et al.*, 2000). A continuous ice-rafted debris (IRD) record from the BDF provides evidence for a dynamic, regional, marine-calving ice sheet in the region, from ~46 to ~12 ka (Scourse *et al.*, 2009).

An improved and spatially consistent understanding of the behaviour of the last BIIS has been aided in part by the availability of high-resolution bathymetric coverage of the Irish shelf acquired for the INFOMAR programme (Cullen, 2003), which has been critical in contextualizing interpretations of less extensive bathymetric surveys (King *et al.*, 1998) and has contributed to an improved and spatially consistent understanding of last BIIS behaviour. In addition, the deglacial history of both the marine and the terrestrial sectors of the last BIIS has been constrained in some detail (e.g. Bowen *et al.*, 2002; Bradwell *et al.*, 2008; Greenwood and Clark, 2009a; Clark *et al.*, 2012, 2018; Callard *et al.*, 2018), allowing correlation with records on the Malin Shelf (Callard *et al.*, 2018; Ó Cofaigh *et al.*, 2019). Studies of seabed sediment and landforms using shallow cores and geophysical data have indicated that the western margins of the last BIIS reached the continental shelf edge in most areas (Scourse *et al.*, 2009; e.g. Benetti *et al.*, 2010; Dunlop *et al.*, 2010; Ó Cofaigh *et al.*, 2012; Bradwell and Stoker, 2014; 1998) except west of central Ireland where it reached the mid-shelf (McCarron *et al.*, 2018). The extension to maximum limits along the Malin Shelf is thought to have occurred relatively early in the Late Devensian (~27 ka) (Ó Cofaigh *et al.*, 2019).

\*Correspondence: Kieran F. Craven, as above.  
E-mail: cravenk@tcd.ie

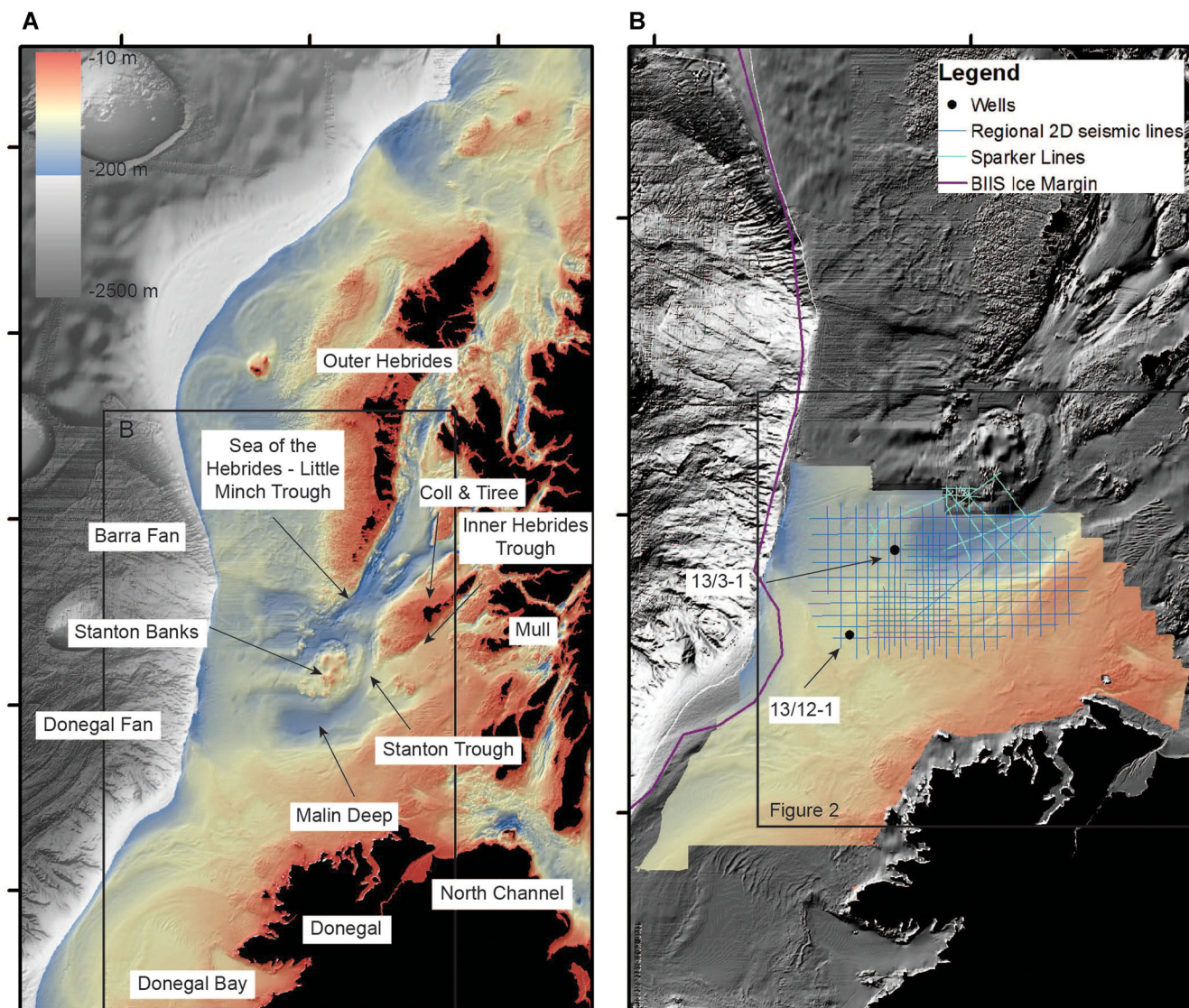


**Figure 1.** (A) Regional bathymetry with geographical locations referred to in the text. (B) Coverage of INSS multibeam bathymetry used in this study (coloured as per panel A), with locations of multichannel seismic profiles (dark blue lines), MESH sparker profiles (turquoise lines) and regional BISS ice extent at the LGM from Clark *et al.* (2012). Black dots show exploration wells used to constrain the bedrock horizon in this study. Bathymetry data beyond INSS limits are from EMODnet and used for illustrative purposes only. [Color figure can be viewed at [wileyonlinelibrary.com](https://onlinelibrary.wiley.com)]

Current reconstructions of the Malin Shelf sector of the BISS indicate that initial deglaciation from a maximum position on the shelf edge at 26.7 ka BP was underway by 25.9 ka BP, with most of the shelf deglaciated by 23.2 ka BP (Callard *et al.*, 2018). Rapid ice margin retreat across the shelf was marked by a lack of well-defined moraines recording significant still-stands (Dowdeswell *et al.*, 2008; Howe *et al.*, 2012; Callard *et al.*, 2018; Clark *et al.*, 2018). A rapid decline in IRD on the BDF during later stages of Termination 1 (Knutz *et al.*, 2001) supports a model of rapid tidewater ice stream retreat focused along submarine troughs on the mid- to outer shelf (e.g. Small *et al.*, 2017), with more stable ice sheet configurations within confined valleys on the inner shelf (e.g. Small *et al.*, 2017; Arosio *et al.*, 2018). Recent dates from the inner shelf further refine the geochronology and dynamics of deglaciation, with topographically constrained ice flow near Tiree (Fig. 1) occurring by  $17.5 \pm 1.0$  ka, and complete deglaciation of the marine sector of the local ice stream by 17–16 ka (Small *et al.*, 2017).

In Scotland, the western sectors of the last BISS are frequently portrayed as a single ice stream occupying the Malin Shelf (e.g. Dunlop *et al.*, 2010; Howe *et al.*, 2012; Ó Cofaigh *et al.*, 2012). However, recent work indicates that multiple ice streaming

events occurred during ice sheet extension offshore, along several inner-shelf valleys and troughs from c. 32 ka (Howe *et al.*, 2012, 2015; Finlayson *et al.*, 2014; Dove *et al.*, 2015), ceasing by  $20.6 \pm 1.2$  ka (Small *et al.*, 2017). In Ireland, terrestrial ice flow indicators indicate ice movement across Malin Head onto the shelf (Greenwood and Clark, 2009b). Drumlinoid features (associated with ice streaming) exist at seabed near Tory Island (Benetti *et al.*, 2010), with indications of the formation of a post-streaming marine embayment in the ice sheet along the north Donegal coast by 22–21 ka (Wilson *et al.*, 2019).

Although these and previous studies provide evidence for ice convergence from multiple sources, current models of the last BISS do not attempt to reconstruct the pattern or timing of these individual ice stream extensions across the Malin Shelf. Interpretations of multibeam bathymetry in inner shelf regions have led to an improved understanding of the pattern and relative timing of individual ice streams contributing to the Malin Shelf (Howe *et al.*, 2012; Dove *et al.*, 2015, 2016; Small *et al.*, 2017), but it remains unclear how they interacted during deglaciation. The operation of cross-shelf extending ice streams provides significant details in our understanding of the last BISS, as these high flux ice flow corridors discharge

large ice volumes and thus play an important role in the overall stability of an ice sheet (e.g. Bamber *et al.*, 2000; Pollard and DeConto, 2009) and are recognized as having influenced both the pattern and the rate of BIIS deglaciation (Eyles and McCabe, 1989; Clark *et al.*, 2012). However, spatiotemporal patterns of ice flow due to the interaction of two or more ice streams across an area of weakly constrained basal flow, such as the sediment-rich Malin Shelf, remain poorly understood (Sayag and Tziperman, 2011). This is especially pertinent given recent modelling and empirical work indicating the importance of buttressing and trough geometry to ice stream behaviour (Sejrup *et al.*, 2016; Gandy *et al.*, 2018).

The aim of this study is to address the gap in knowledge about the relative chronology of BIIS ice streaming in the area of the Malin Shelf. This is addressed by integrating high-resolution multibeam acoustic bathymetric data with legacy geophysical datasets of varying spatial and vertical resolutions (sub-bottom, sparker and multichannel seismic profiles) in the area south of the Stanton Banks (Fig. 1a). These integrated data allow a new characterization of the glacial geomorphology and seismic stratigraphy of the area, including both seafloor and buried landforms, contextualizing and linking previous studies on the inner- and shelf edge (e.g. Knutz *et al.*, 2001; Wilson and Austin, 2002; Scourse *et al.*, 2009). The results provide evidence for the extent, interaction and relative chronology of Scottish and Irish BIIS ice streams on the Malin Shelf, affording new insights into the dynamic interactions of adjacent ice sheet sectors during deglaciation, and offers a physical analogue for the interaction of ice streams in the marine-based sectors of modern ice sheets.

## Regional setting

### *Regional physiography and geology*

The Malin Shelf spans an area that extends approximately 150 km north from the Irish coast to the Outer Hebrides, and 200 km west from the Scottish coast to the shelf edge (Fig. 1). The shelf break is located in water depths of about 200 m and the continental slope descends sharply to depths of up to 2800 m in the Rockall Trough. The slope of the Rockall Trough is marked by two large-scale features, the Donegal Fan west of the Malin Shelf and the Barra Fan north of the Stanton Bank, commonly referred to as a single fan complex extending over an area of 10 000 km<sup>2</sup> (Fig. 1). The BDF is a Plio-Pleistocene sediment wedge up to ~650 m thick, and represents the largest deposit of glacial sediment on the western British and Irish continental margin (Armishaw *et al.*, 1998; Torbjørn Dahlgren *et al.*, 2005).

The ~13 000-km<sup>2</sup> study area is located in the south-western sector of the Malin Shelf, south of the Stanton Banks, and contains water depths ranging from 50 to 200 m (Fig. 1b). The area lies mainly (85%) within the Irish sector of the Malin Shelf and is covered by high-resolution multibeam bathymetry and sub-bottom (SB) profiles obtained between 2003 and 2004 during the Irish National Seabed Survey (INSS) programme (Cullen, 2003).

Several prominent bathymetric lows occur within and to the north of the study area, including the 'Malin Deep', the 'Stanton Trough', the 'Sea of the Hebrides–Little Minch Trough' and the 'Inner Hebrides Trough' (Fig. 1a). The lows coincide with regional structural features, and are thought to reflect prolonged glacial erosion in the region (Fyfe *et al.*, 1993). However, due to a westward thickening of Quaternary sediment cover (up to of 285 m thick along the shelf edge) no bedrock outcrops at the seabed surface. Beneath the

sediment cover the area is floored by Carboniferous, Jurassic and late Mesozoic sedimentary rocks cut by Tertiary sills and dykes (Fyfe *et al.*, 1993). The northern limit of the study area is bounded by a ridge of Lewisian and Torridonian basement rocks which extends from the Scottish mainland onto the Stanton Banks and is crosscut by the Stanton Trough (Evans *et al.*, 1980; Fyfe *et al.*, 1993).

### *Quaternary stratigraphy*

Studies of the broad Hebridean Shelf to the north of the study area (Fig. 1) provide evidence of cross shelf glaciation since the mid-Pleistocene transition (MIS12, c. 0.44 Ma) (Stoker, 1995). Offshore evidence of BIIS extension from western Scotland and northern Ireland onto the Malin Shelf includes bedrock erosion, over-deepened trenches, shelf edge moraine-like ridges and deep-water IRD records (Knutz *et al.*, 2001; Scourse *et al.*, 2009; Dunlop *et al.*, 2010; Howe *et al.*, 2012). Previous studies in the Malin Shelf region using seismic profiles and cores have identified six main Quaternary sediment units interpreted to be of both glacial and glaciomarine origin (Table 1), interpreted to record at least two cycles of glacial occupation of the shelf: the older of pre-Late Devensian age based on stratigraphic position below a shelf-wide erosion surface (Davies *et al.*, 1984) and amino acid dating (Fyfe *et al.*, 1993); and the younger of Late Devensian age based on radiocarbon dates (e.g. Binns *et al.*, 1974; Callard *et al.*, 2018).

Of these six, the Skerryvore Formation has been identified as the oldest Quaternary sediment package in the region, pre-Devensian in age and comprising stiff silty clays up to 70 m thick deposited during a period of deteriorating temperate to glacial climate (Davies *et al.*, 1984; Fyfe *et al.*, 1993). Seismically, it has low internal backscatter with a structureless basal unit and thinner upper unit with faint horizontal parallel bedding (Davies *et al.*, 1984) (Table 1).

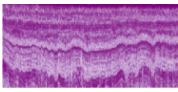
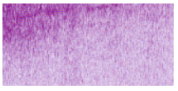
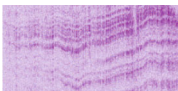
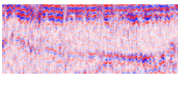
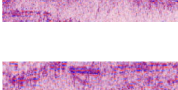
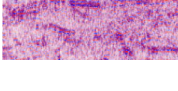
The Malin Formation unconformably overlies the Skerryvore Formation with an average thickness of 75 m (Fyfe *et al.*, 1993) and consists of two units. The lowermost Malin A is seismically structureless and interpreted as a subglacial till, while the overlying Malin B (found in small, isolated pockets in this study) contains parallel sub-horizontal reflectors interpreted to be glaciofluvial or glaciolacustrine in origin (Davies *et al.*, 1984). The Malin Formation can have a mounded cross-sectional geometry (Davies *et al.*, 1984; Fyfe *et al.*, 1993) with a wide distribution across the study area (Dunlop *et al.*, 2010).

The Canna Formation unconformably overlies the Malin Formation, has a maximum thickness of 50 m and is largely acoustically transparent (Davies *et al.*, 1984). It is composed of sands, silts and clays with numerous pebbles and cobbles (Fyfe *et al.*, 1993). While previously interpreted as glaciomarine in origin (Davies *et al.*, 1984), strong similarities with the younger Barra Formation (described below) suggests a reinterpretation is required.

The Stanton Formation unconformably overlies the Canna Formation in thicknesses up to 120 m. It is well stratified with parallel and draping reflectors that can be traced over several kilometres. The Stanton Formation comprises stiff laminated clay interpreted as glaciomarine in origin and of pre-Late Devensian age (Davies *et al.*, 1984; Fyfe *et al.*, 1993). It has been identified on SB profiles within the Malin Deep (Dunlop *et al.*, 2010).

A major cross-shelf erosion surface truncates the Stanton and several stratigraphically lower formations. The relatively smooth surface has been shown to grade onto bedrock in inner shelf areas and terminates at the shelf break (Davies *et al.*, 1984; Callard *et al.*, 2018). Both these studies interpret it to have formed by subglacial erosion beneath the last BIIS during the Last Glacial Maximum (LGM).

**Table 1.** Seismic unit descriptions and interpretations.

Seismic unit <sup>5</sup>	Seismic character <sup>5</sup>	Image <sup>5</sup>	Correlated formation	Interpreted depositional environment	Distribution	Inferred age <sup>1, 2, 3, 5</sup>	Interpreted geomorphology <sup>5</sup>
S6	Seabed sands Stratified drape		Jura <sup>1, 2, 3, 4</sup>	Erosional lag Glaciomarine <sup>1, 2</sup>	Shelf wide Malin Deep; NW shelf <sup>3, 5</sup>	MIS 1 MIS 2 Termination 1 (<24 ka)	
S5	Transparent		Barra <sup>1, 2, 3, 4</sup>	Subglacial to ice proximal <sup>4</sup> glaciomarine <sup>1, 2</sup>	Shelf wide <sup>3, 5</sup>	MIS 2 (27–24 ka)	GZWs MSGSL Lateral shear-moraine
R2 S4	Stratified		Stanton <sup>1, 2, 3</sup>	Erosion surface <sup>1, 2, 3</sup> Glaciomarine <sup>1, 2</sup>	Shelf wide <sup>1, 5</sup> Malin Deep <sup>3, 5</sup>	MIS 2 (27–24 ka) MIS 4–12?	Eroded channels
S3	Transparent		Canna <sup>1, 2</sup>	Glaciomarine <sup>1, 2</sup>	Malin Deep <sup>5</sup>	MIS 4–12?	Eroded channels
S2	Stratified		Malin B <sup>1, 2</sup>	Glaciofluvial <sup>1, 2</sup>	Shelf wide <sup>1, 2, 3, 5</sup>	MIS 4–12?	Eroded channels MSGSL Drumlinoid features
	Transparent		Malin A <sup>1, 2</sup>	Subglacial <sup>1, 2</sup>			
S1	Semi-transparent		Skerryvore <sup>1, 2</sup>	Marine to glaciomarine <sup>1, 2</sup>	Malin Deep <sup>5</sup>	< MIS 12?	
R1				Erosion surface <sup>1, 2</sup>		MIS 12?	

<sup>1</sup> Davies *et al.* (1984);<sup>2</sup> Fyfe *et al.* (1993);<sup>3</sup> Dunlop *et al.* (2010);<sup>4</sup> Arosio *et al.* (2018);<sup>5</sup> this study.

The erosion surface is overlain by two units, the Barra and Jura Formations (Davies *et al.*, 1984; Fyfe *et al.*, 1993; Dunlop *et al.*, 2010). The lowermost Barra Formation is found across the inner and outer Malin Shelf (Dunlop *et al.*, 2010), varying in thickness from a few metres to up to 130 m (Davies *et al.*, 1984). It is similar in character to the Canna Formation, with a generally low internal seismic reflectivity and occasional randomly spaced internal reflectors. Originally interpreted as a deglacial glaciomarine unit (Davies *et al.*, 1984), recent work has indicated that the Barra Formation should be reinterpreted as a time-transgressive, sub-glacial to ice-proximal sediment package, containing grounding zone wedges (GZWs) on the mid-shelf (Arosio *et al.*, 2018).

The Jura Formation is up to 300 m thick and deposited on underlying units or bedrock. It is well stratified with closely spaced, parallel horizontal to inclined reflectors (Davies *et al.*, 1984). The formation thickens towards the coast, with acoustic blanking due to the presence of gas commonly observed. It is interpreted as glaciomarine in origin (Davies *et al.*, 1984; Fyfe *et al.*, 1993) and of a Late Devensian to Holocene age (post 16.5 ka; Fyfe *et al.*, 1993; Szapak, 2012).

## Data and Methods

The study area (Fig. 1b) contains a variety of legacy geophysical data including multibeam swath acoustic bathymetry and seismic profiles of varying frequency content. Multibeam and SB acoustic profiles were acquired in 2003–2004 during the INSS programme (Cullen, 2003). Sparker profiles were acquired as part of the 2005 Mapping European Seabed Habitats (MESH) survey (Wallis, 2006).

Multichannel Seismic (MCS) profiles were acquired by Fugro-Geoteam AS in 1999.

## Geophysical datasets

Multibeam data were acquired by the RV *Celtic Explorer* using a hull-mounted Kongsberg-Simrad EM1002 multibeam echo sounder with an operational frequency of 93–98 kHz (e.g. Zhilin and Sheridan, 2003), yielding a vertical resolution of 0.1–0.5 m depending on water depth. Data were processed using CARIS HIPS and SIPS v9.1, with depth referenced to the lowest astronomical tide (LAT).

SB profiles were acquired across the study area concurrently with multibeam data, using a hull-mounted SES Probe 5000 3.5-kHz system yielding a theoretical vertical resolution of 0.2–0.5 m (Zhilin and Sheridan, 2003). Mainline spacing is approximately 0.5 km, with crossline spacing of approximately 7 km.

Sparker profiles (Fig. 1b) were acquired by the RRS *Charles Darwin*. The source was an EG&G, nine-candle array with 135 tips supplied from a CSP 2200 HV capacitor discharge unit, generally running at 1700 J per pulse, with a Teledyne 10 m, seven-channel streamer (Wallis, 2006). A bandpass filter of 100–1730 Hz was applied with vertical resolution <0.3 m.

MCS profiles were acquired for hydrocarbon exploration and obtained under licence from the Government of Ireland Petroleum Affairs Division. Data were processed by the original acquisition team using a standard sequence of stack, deconvolution and 2D migration. A low-cut band filter of 3.5 Hz and high-cut of 309 Hz were applied. Peak frequency contents of 10<sup>1</sup> Hz correspond to a seabed vertical resolution of 5–10 m in water depths of 150–200 m.

## Interpretation methods

Edited (cleaned) multibeam bathymetric data were gridded in Fledermaus Dmagic v7.5 and exported into ArcGIS v10.3 for further analysis as a 10-m horizontal resolution Digital Elevation Model (DEM). To highlight surface features, relief-shaded terrain models were generated using the 'RVT' multi-directional shading toolkit, which composites illuminations from eight different azimuths to remove observational bias (Kokalj *et al.*, 2011; Zakšek *et al.*, 2011). The incident light elevation angle was set at 10°. Bathymetric positioning indices (BPIs) were calculated after Wilson *et al.* (2007) by subtracting the mean raster value within a circle of given radius from the cell bathymetric value to analyse seafloor landforms. BPIs are scale-dependent and, following visual comparison of BPIs based on a range of 750–10 cells, we chose floating point values from a circular radius of 500 and 100 cells (i.e. 5000 and 1000 m, respectively).

SB, sparker and MCS profiles were all interpreted using standard techniques of seismic stratigraphic analysis, based on the definition of units using discordant reflector relations and internal facies character (e.g. Cross and Lessenger, 1988). Observations were made regarding the external geometry (e.g. sheet, drape, wedge, mound) and internal reflection composition (e.g. reflector continuity, configuration and amplitude) of these units. A stratigraphy was established by correlating units with previously described seismic stratigraphies, based on their geographical distribution, stratigraphic position and seismic facies character (Davies *et al.*, 1984; Fyfe *et al.*, 1993; Dunlop *et al.*, 2010) and correlation of the units to two exploration wells to constrain the bedrock horizon within the study area (Stuart, 1979; Craig and Welding, 2006) (Fig. 1b).

SB, sparker and MCS profiles were interpreted using CodaOctopus Survey Engine v5.4. Interpreted horizons were exported as sets of points (XYZ) comprising depths below seabed calculated assuming a seismic velocity of 1650 m s<sup>-1</sup> in all units (Szpak *et al.*, 2012). Points were imported to ArcGIS for further analysis and sub-seabed horizons were calculated using the previously created 10-m seabed DEM. Interpolation of the surfaces used ordinary kriging, with a spherical semivariogram model and output cell size of 250 m; a variable search radius of 12 points was applied. In total, we interpreted 176 SB profiles (69 N–S, 107 E–W; line spacing ~ 3 km; Supporting Information, Fig. S1), 14 sparker profiles (nine N–S, five E–W; line spacing ~7 km) and 48 MCS profiles (28 N–S, 20 E–W; line spacing ~4 km). Selected profiles are presented in Fig. 2.

## Results

This study uses multibeam echosounder (MBES) data (Fig. 1) to identify seafloor glacial landforms, and seismic profiles (Fig. 2) to identify stratigraphic units and buried landforms within them (Figs 3–5). High-frequency profiles (SB and sparker) are used to identify and trace individual units. MCS profiles of lower frequency content, which are less affected by signal attenuation at depth or the presence of gas, are used to trace major reflectors across the study region, constrained by boreholes and intersecting high-frequency profiles where possible.

We identify six seismic units (labelled S1–S6 from bottom to top) above bedrock within the Malin Deep (Fig. 1) and adjacent areas of the south-west Malin Shelf (Table 1). The thicknesses of individual units range from approximately 10 to 80 m. All six units are observed on sparker profiles within the Malin Deep, although only S2 and S5 are observed outside of

this topographic and bedrock low. Only four shallower units (S2, S4–S6) are identified on lower penetration SB profiles within the Malin Deep. Most units have a consistent internal seismic character, with the exception of S5 which varies spatially across the study region (see below).

Two major reflectors are identified: R1 separates sediment units from bedrock, while R2 separates S5 and S6 from underlying units. We first summarize the distribution and character of seismic units across the study area, then describe selected seabed and buried landforms.

## Description and correlation of seismic units

Following previous studies, the Malin Shelf contains evidence of at least two glacial cycles of overall advance and retreat comprising (i) grounded ice advance and subglacial erosion followed by (ii) sub- to pro-glacial deposition of sediments in marine settings. R1 is interpreted to be the bedrock surface, as verified by bedrock depth in two existing boreholes (Fig. 1). R2 is the erosive base of Late Devensian (LGM) ice expansion onto and across the shelf. We interpret four seismic units formed during at least one glacial cycle of unidentified age to be bounded between the principal reflection horizons R1 and R2, with the deposits and seabed landforms of the second glacial cycle located above R2 being Late Devensian in age. The six seismic units (S1–6) identified are correlated to previously identified stratigraphic formations in the area to infer their ages and depositional environments (Table 1).

S1, the lowermost unit, is identified on sparker profiles and found within the central axis of the Malin Deep (Fig. 3d). S1 unconformably overlies bedrock (R1 truncating underlying reflectors) and varies in thickness, being absent in places, and up to ~ 50 m thick in a bedrock depression. Internally, it is characterized by faint wavy to horizontal stratification. Its top surface is sub-horizontal and does not form constructive topography. Based on its stratigraphic position and seismic character, we correlate S1 with the pre-Devensian Skerryvore Formation.

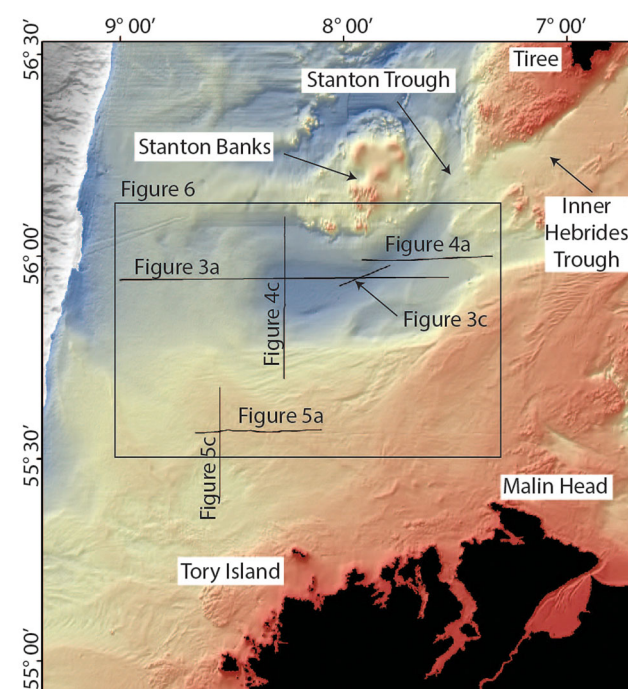


**Figure 2.** Bathymetric data overlain with locations of seismic profiles displayed in subsequent figures, along with key locations referred to in the text. Bathymetric data below 200 m water depth are from EMODnet. [Color figure can be viewed at [wileyonlinelibrary.com](http://wileyonlinelibrary.com)]

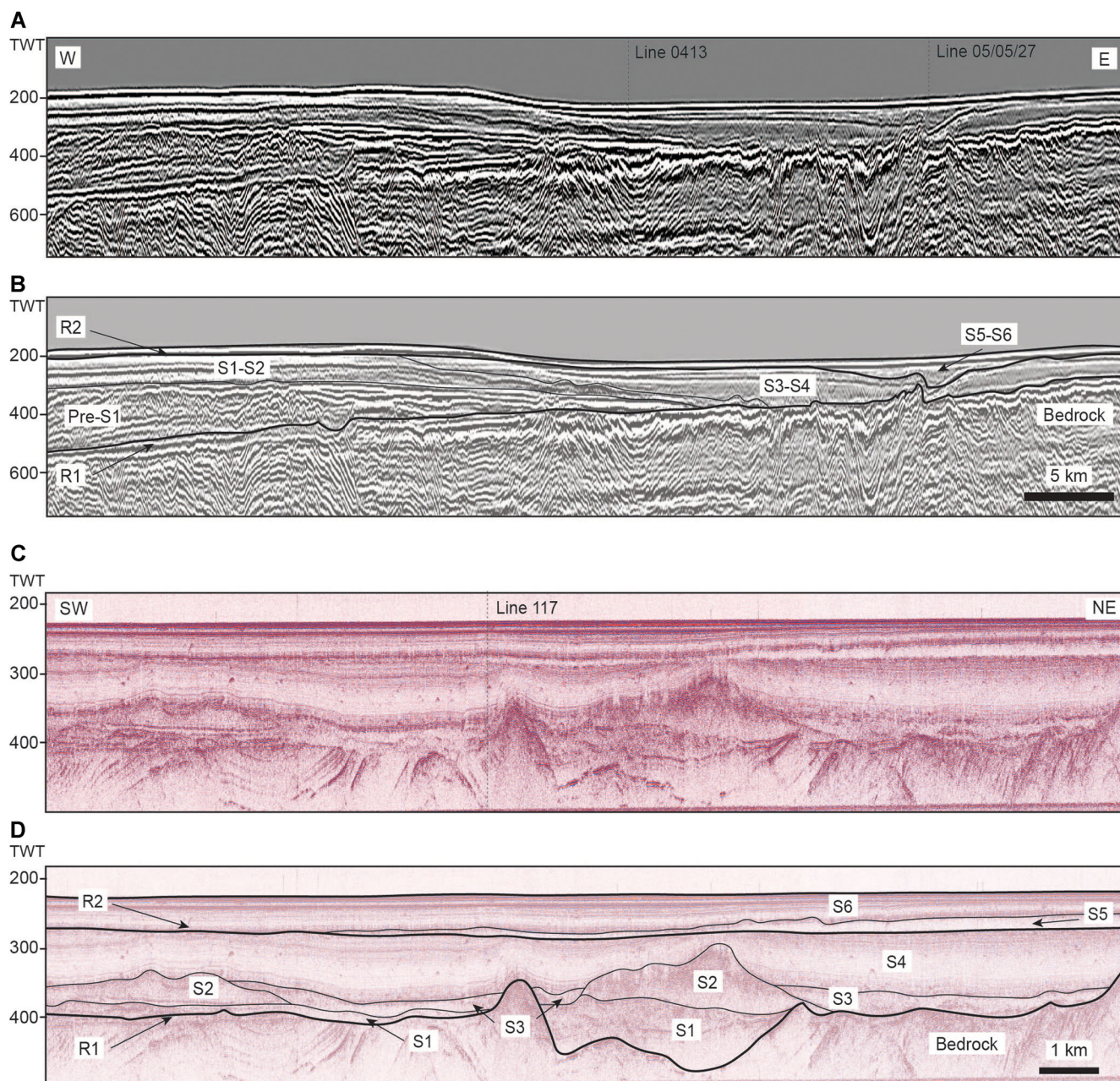


**Figure 3.** Seismic profiles – see Fig. 2 for locations. (A) Multichannel seismic profile Line 117 running west to east from the outer continental shelf to the Malin Deep. (B) Interpretation of Line 117. (C) Sparker seismic profile 05/05/27c running south-west to north-east along the axis of the Malin Deep. (D) Interpretation of profile 05/05/27c. R1 = bedrock horizon; R2 = LGM erosion surface; S1 = Skerryvore Fm; S2 = Malin Fm; S3 = Canna Fm; S4 = Stanton Fm; S5 = Barra Fm; S6 = Jura Fm (see text for description and correlation of seismic units to previously described formations). Vertical scale is two-way travel time (TWT) in milliseconds. [Color figure can be viewed at [wileyonlinelibrary.com](http://wileyonlinelibrary.com)]

S2 is observed on seismic profiles in and adjacent to the Malin Deep as a laterally discontinuous unit with a strongly reflective, upper surface that forms discrete, multi-crested irregular mounds up to 75 m thick (Fig. 3d). S2 is separated from S1 by a smooth to irregular strong reflector. On SB profiles, S2 is acoustically transparent with no internal structure, both within the Malin Deep and to the south and east where it locally outcrops. S2 forms a large proportion of the subsurface sediment underlying the plateau area flanking the depression (Fig. 3b) with thicknesses up to 80 m on this eastern and southern margin of the Malin Deep and chaotic internal reflectors. We correlate S2 with the pre-Late Devensian Malin Formation based on its stratigraphic position and mounded cross-sectional geometry character in and adjacent to the Malin Deep. While the Malin Formation includes two seismic facies, in our seismic profiles S2 is generally unstratified, except for dipping reflections observed on MCS (Fig. 3b).

S3 is identified only on sparker profiles within the Malin Deep. It is an acoustically transparent unit up to 25 m thick but is laterally discontinuous. It lies unconformably above S2, S1 and bedrock (Fig. 3d). S3 onlaps S2 and is consistently draped by S4. We correlate S3 with the pre-Late Devensian Canna Formation based on its stratigraphic position and seismically transparent nature.

S4 is observed only within the Malin Deep as a laterally continuous unit up to 70 m thick draping S3, S2 and bedrock. Internally, it is finely stratified with folded layering that is truncated against a sharp upper reflector R2 (Figs 3 and 4). Point source diffraction patterns are present, with higher densities of reflectors occasionally along internal horizons. We correlate S4 to the pre-Late Devensian Stanton Formation based on its stratified character, distribution within the Malin Deep, stratigraphic position and truncation by R2, the Late Devensian LGM erosion surface.

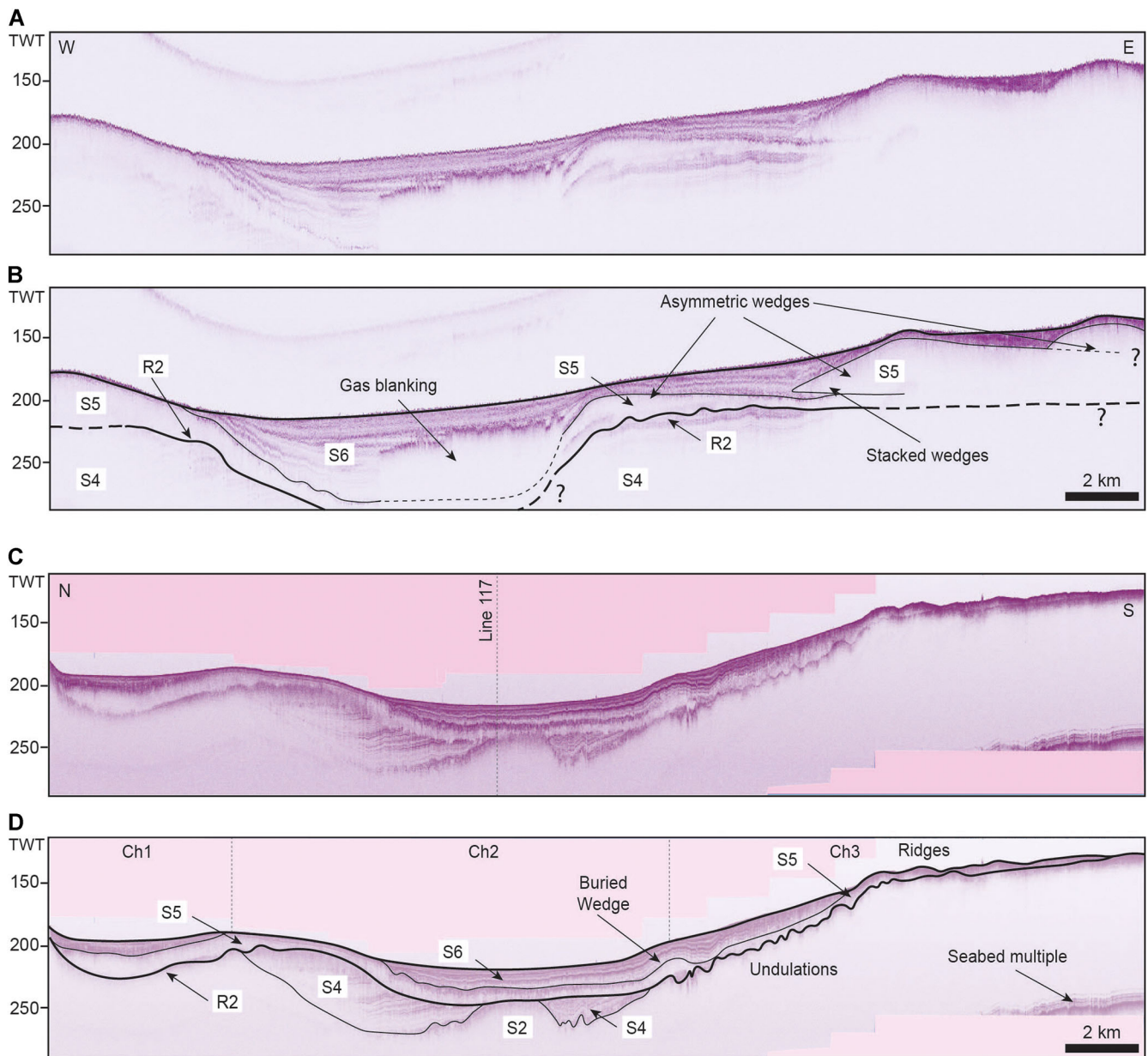


**Figure 4.** Sub-bottom profiles – see Fig. 2 for locations and interpretive nomenclature as in Fig. 3. (A) SB Profile 0128 running west to east across the junction of the Stanton Trough to the north and Malin Deep to the south, near the mouth of the Inner Hebrides Trough. (B) Interpretation of SB Profile 0128. Note: (i) the central depression cut into S4 by R2; (ii) above R2, S5 forms a stacked series of asymmetrical wedges that thicken towards the central depression – the wedges interfinger and are draped by S6 which infills the depression; (iii) the wedges of S5 also appear to create mounds at the seabed with distance from the central depression. (C) SB Profile 0413 running north–south across the Malin Deep. (D) Interpretation of SB Profile 0413. Note: (i) Multiple infilled depressions (Ch1–3) within the sediment sequence (Supporting Information, Fig. S2); (ii) a set of regularly spaced sub-kilometre-scale undulations along R2 (labelled); and (iii) wedges in S5 forming constructive topography at depth separating infilled depressions and forming ridged topography at the seabed. [Color figure can be viewed at [wileyonlinelibrary.com](http://wileyonlinelibrary.com)]

S5 is a laterally continuous sedimentary unit that extends across almost the entire shelf although absent from parts of the central Malin Trough and the area to the south. S5 is generally 15 m thick and internally transparent (similar to S3), but adjacent to the Malin Deep contains irregular internal reflections that define several stacked units up to 30 m thick (Figs 4–7). S5 overlies S4 within the Malin Deep, and overlies S2 outside the Malin Deep. The base of S5 is defined by R2, the shelf-crossing unconformity that truncates S4 and lower units and forms an irregular corrugated surface (Fig. 4d). Within the Malin Deep, the upper surface of S5 is generally smooth but does form constructive topography; outside of the Malin Deep this upper surface forms elongate mounds at the seabed (Fig. 4d). We correlate S5 to the Late Devensian Barra Formation based on its low internal seismic reflectivity, stratigraphic position and extensive distribution; we identify

S5 across all shelf sectors apart from the central axis and margins of the Malin Deep. The sub-ice to ice-proximal depositional environment interpretation of Arosio *et al.* (2018) is supported in this study by the composite sediment packages and seafloor ice proximal to subglacial landforms.

The final unit, S6, is laterally continuous but spatially confined to the Malin Deep where it onlaps and interfingers with S5 (Fig. 3). Where S5 is absent (along the axis of the Malin Deep and on the flanks of the Stanton Banks), S6 drapes S4 and occasionally bedrock. S6 is generally ~ 30 m thick but thickens to 70 m in parts of the Malin Deep. S6 is a well-stratified unit with parallel, sub-horizontal reflectors (comparable to the undulating reflectors in S4), that includes at least one prominent internal unconformity. Gas blanking is common where the unit is thicker (Fig. 4). We correlate S6 with the stratified Late Devensian to Holocene glaciomarine Jura

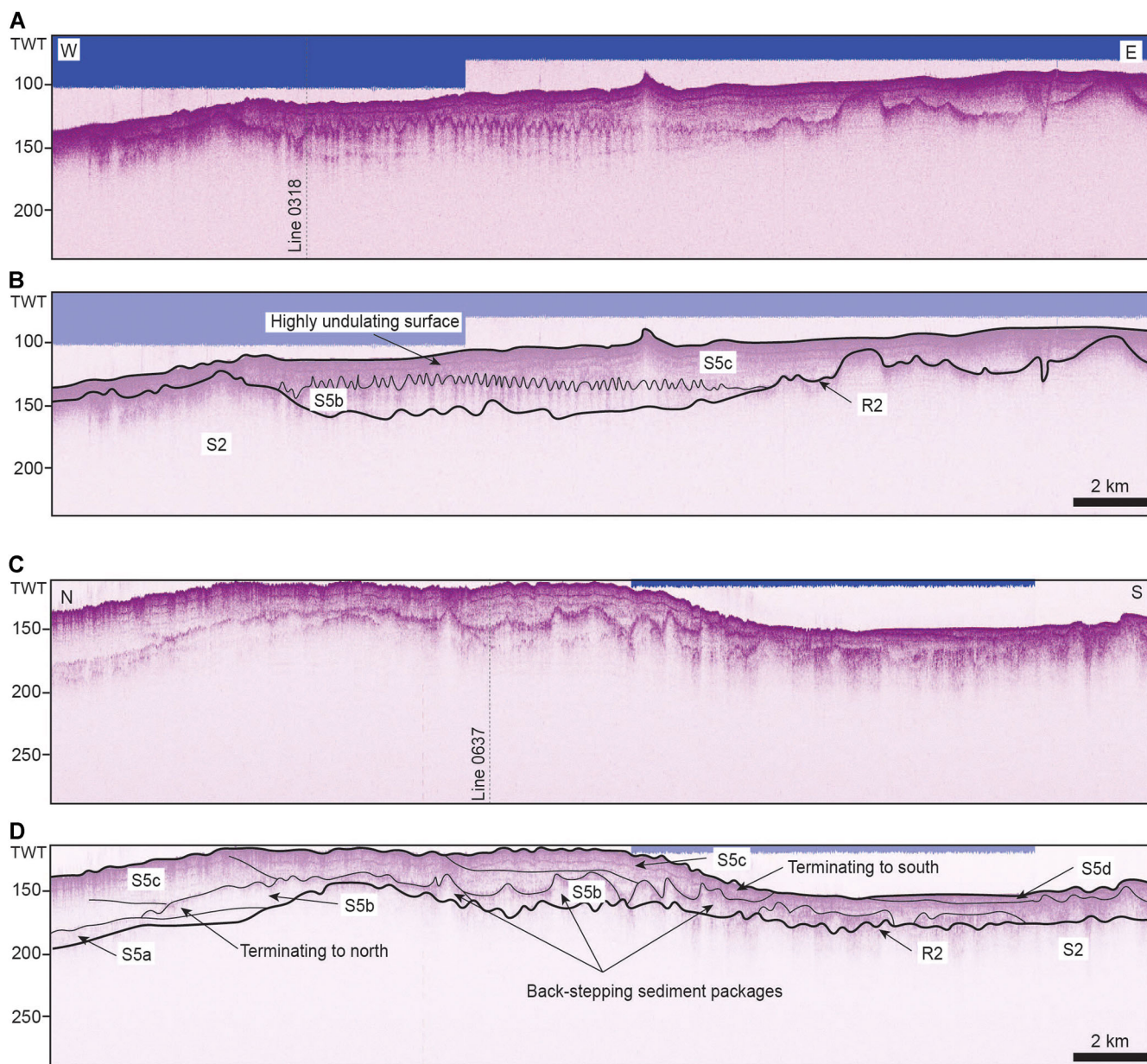


**Figure 5.** Sub-bottom profiles – see Fig. 2 for locations and interpretive nomenclature as in Fig. 3. (A) SB Profile 0637 running west–east across a broad bathymetric high (platform 85–96 m below sea level) south of the Malin Deep. (B) Interpretation of SB Profile 0637. Note: (i) a shallow NW-trending buried depression cut in S2 along R2; (ii) the regularly undulating surface of S5b, with topographic crests of buried mounds spaced ~ 300 m apart across an area of ~16 km. (C) SB Profile 0318 running N–S. (D) Interpretation of SB Profile 0318 with stacked irregular wedges within S5b which pinch out northwards over an irregular R2 surface. S5 extends to the seabed, forming a broad bathymetric high with an undulating seabed profile that pinches southwards. [Color figure can be viewed at [wileyonlinelibrary.com](http://wileyonlinelibrary.com)]

Formation based on its highly stratified character, distribution within the Malin Deep and stratigraphic position.

### Description of buried and seafloor landforms

The Malin Shelf contains landforms both at the seabed and buried within the sediment cover, some of which are described here for the first time. Multibeam data provide information on seafloor features (Fig. 2), while the available grid of seismic reflection profiles allows the mapping of the bedrock surface (R1) and a prominent sediment erosion surface (R2), as well as providing information on the internal character of seafloor and buried features. We are mainly concerned with buried landforms within S5; buried landforms are observed within older (pre-LGM) units in some profiles (e.g. Fig. 3), but are not the focus of this study.

### Buried landforms

The map of R1 (bedrock surface) interpolated from MCS profiles reveals the presence of a cross-shelf, flat-floored depression, occurring at depths between 50 and 350 m below the current water surface, 60 km long by up to 40 km wide that widens westward to form a seaward-facing embayment (Fig. 6a). Several sinuous generally east–west orientated linear depressions are incised along the base of the embayment and are also cut into the shelf to the south. All seismic units described above are deposited within this embayment.

The map of R2 (base-LGM surface) interpolated from MCS profiles reveals two linear, subparallel enclosed basins, generally orientated north-east to south-west (Fig. 6b) separated by a medial bathymetric high. The larger, northern basin narrows northwards towards the Stanton Trough, outside of the study area, while the smaller, narrower southern basin pinches out north-east

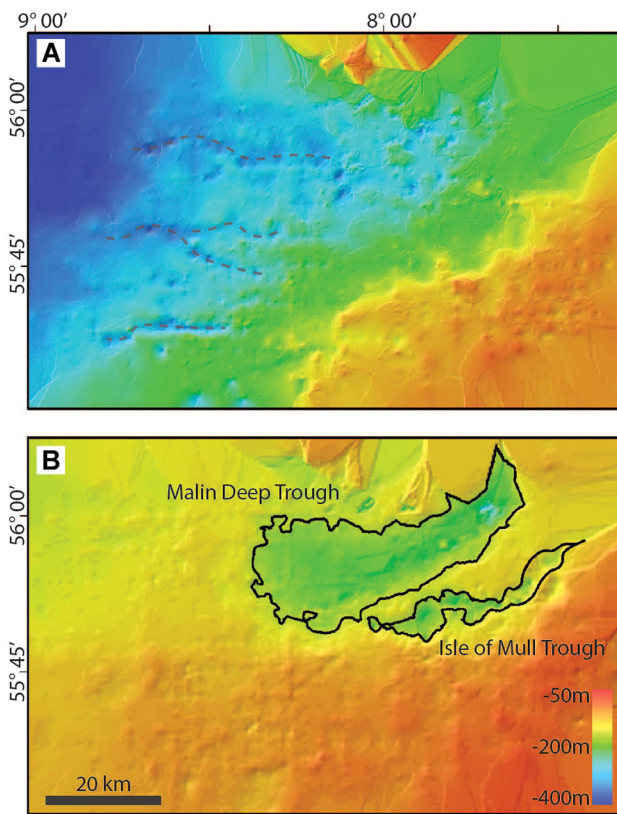


**Figure 6.** Maps of depths below sea level of surfaces gridded from seismic reflection profiles (location of survey area in Fig. 2). Depths are based on an assumed seismic velocity sub-seafloor of  $1650 \text{ m s}^{-1}$ . (A) The R1 (top bedrock) surface (horizon picked from MCS and sparker profiles); note the surface shows a broad, eastward narrowing embayment with cross-shelf sinuous linear depressions (axes indicated by dashed lines). (B) The R2 (base-LGM) surface (horizon picked from MCS, sparker and SB profiles); the 200-m contour outlines two subparallel troughs, here termed 'Malin Deep Trough' and 'Isle of Mull Trough', which correspond to bathymetric depressions (Fig. 2). [Color figure can be viewed at [wileyonlinelibrary.com](http://wileyonlinelibrary.com)]

towards the Inner Hebrides Trough. The basin geometry is observed at higher resolution on some SB profiles with deposition of S6 spatially limited to within these two basins. In the NE of the study region, SB profile 0128 (Fig. 4) crosses the 10-km wide, 55-m-deep larger basin. Here, on the eastern margin, westward thickening asymmetrical buried wedges of S5 are seen to interfinger with thin packages of S6. The S5 unit thicknesses range between 10 and 35 m with observed lateral (east–west) extensions of between 6.5 and 15 km. Westward-facing wedge slopes range from  $0.6$  to  $0.8^\circ$ , with eastward-facing distal slopes range between  $0.1$  and  $0.2^\circ$ .

Further west, SB profile 0413 (Fig. 4d) reveals three channels (Ch1–3) in the R2 surface. Ch1 is the most northern, an east–west-trending depression approximately 6 km wide and 30 m deep that is cut into S2. R2 is draped by S5, which forms a northward-thinning tabular interval up to 20 m thick that extends to the south and is in turn covered by S6, which fills the topographic depression. A larger, east–west-trending depression in R2 occurs to the south of Ch1 (Supporting Information, Fig. S2). This is up to 16 km wide and 30 m deep and is cut into S4 and S2. The depression is subdivided into two smaller depressions (Ch2 and Ch3) by a thickening of S5 to form an asymmetrical feature with a mound-like cross-section geometry. Within the axis of the Malin Deep, S6 drapes the tabular geometry of S5 and infills the bathymetric low formed by its surface draping R2 below. South of this, R2 displays a distinct set of regular undulations over a 9-km-wide

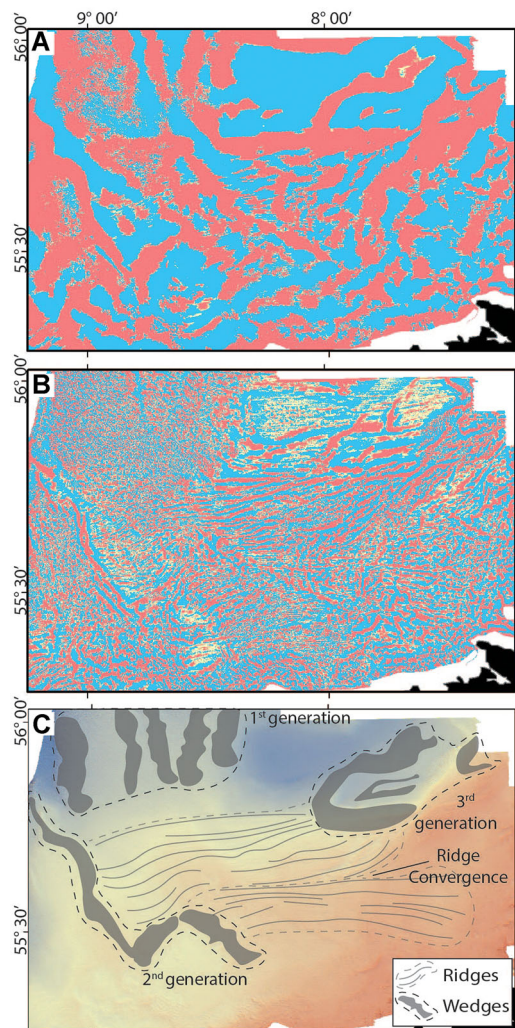


**Figure 7.** Bathymetric Position Index (BPI) analysis of seabed bathymetry (location of area shown in Fig. 8). (A) BPI analysis with 5000-m radius highlighting broad linear highs (wedges) and lows (troughs) across the shelf; bathymetric highs are shown in red, lows in blue. (B) BPI analysis with 1000-m radius revealing smaller geomorphological features, including long curvilinear ridges to the south of the Malin Deep. (C) Map of major landforms mentioned in the text (boundaries indicate limits of related suites of features; three successive generations of grounding zone wedge formation are discussed in the text). [Color figure can be viewed at [wileyonlinelibrary.com](http://wileyonlinelibrary.com)]

zone (Fig. 4d). The undulations have a wavelength of 0.6–0.8 km and crest-to-trough amplitudes of up to 2–3 m.

A further erosional depression containing a similar succession of sediments and top surface morphologies occurs in the SW of the study region. A buried NW-trending, 16-km wide, 30-m-deep depression in the area is infilled by a composite S5 package imaged by SB profile 0637 (Fig. 5). Here, a subunit S5b shows a distinctly undulating top surface reflector. Undulation wavelengths of 200–400 m and amplitudes of 3–5 m occur over a distance of over 10 km. In a correlated longitudinal section, S5b underlies a bathymetric high (Fig. 5d), itself underlain by S2. The S5 composite package back-steps southward along the continental shelf, with an irregular top surface. S5c, a unit with similar acoustic characteristics, is deposited above this, and S5d forms a seabed bathymetric high of c. 10 m before pinching out southwards.

#### Seafloor landforms

The seabed of the Malin Shelf is characterized by multiple sets of intersecting and overlapping ridges separated by intervening

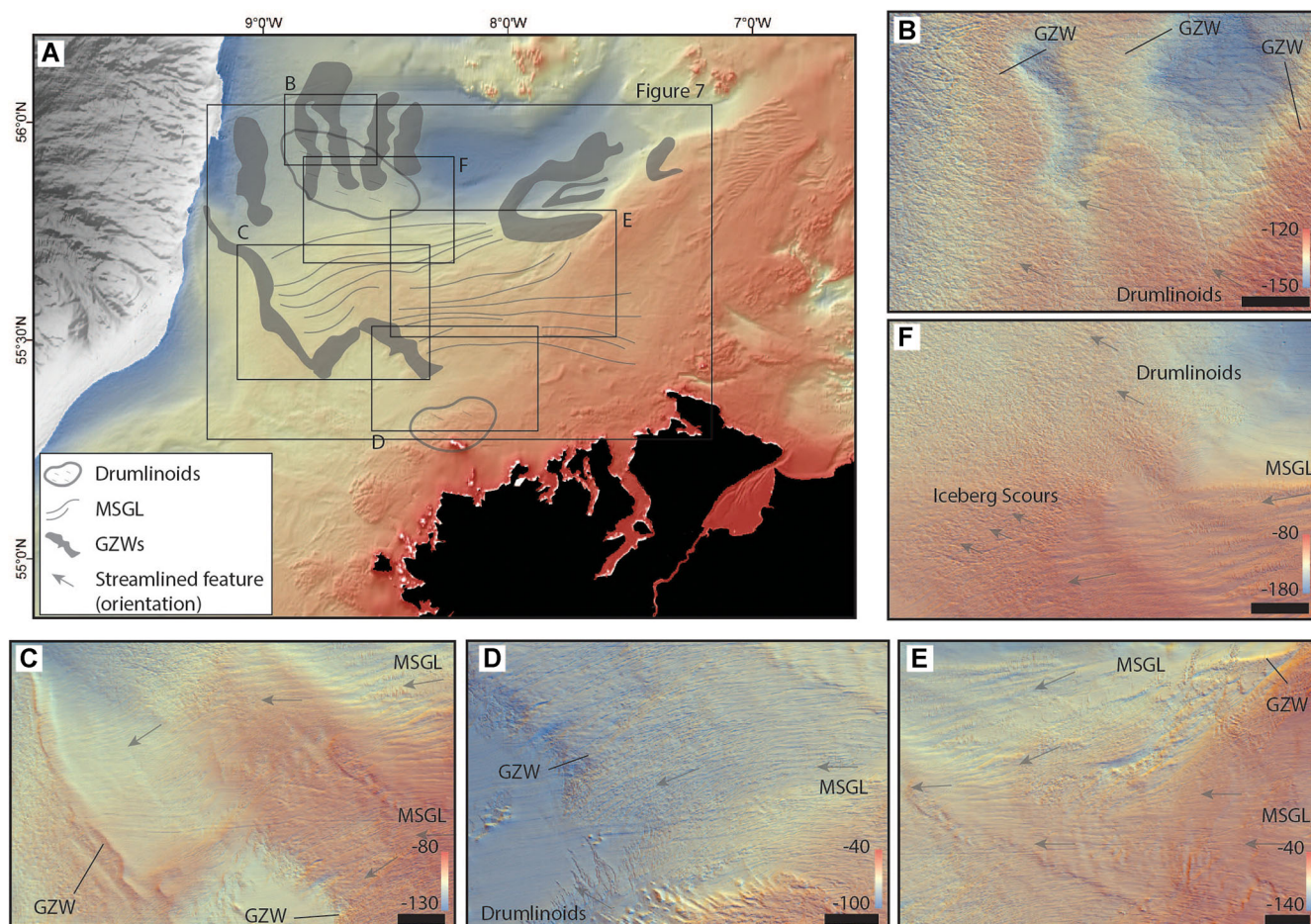


**Figure 8.** Details of seafloor glacial geomorphology from INSS multibeam bathymetric data. Bathymetry colour is for illustrative purposes; depth range changes per panel. Black scale bar is 5 km. (A) Main seafloor glacial landforms as per Fig. 7 (GZWs, MSGLs and ice flow orientation of streamlined features) and extent of previously published streamlined drumlinoids (Benetti *et al.*, 2010; Dunlop *et al.*, 2010). (B–F) Key localities (see text) with seafloor relief highlighted using multi-directional RVT shading (eight sun directions, vertical exaggeration is  $\times 10$ ): (B) overprinted 1st-generation GZWs formed by major ice stream from the north (Sea of the Hebrides Ice Stream – SHIS); (C) 2nd-generation GZWs formed by ice flow from the north-east (Inner Hebrides Ice Stream – IHIS) and east (North Channel Ice Stream – NCIS) with MSGLs located up-ice; (D) 2nd-generation GZW deposited by ice from the east (NCIS) burying streamlined bedrock related to ice flow from Donegal to the south (Tory Island Ice Stream); (E) confluence of MSGLs sets, south of the Malin Deep related to ice flow from the north-east (IHIS) and east (NCIS) – 3rd-generation GZW associated with ice retreat to the north-east (IHIS); (F) an area of streamlined and iceberg-scoured GZWs related to ice flow from the north/north-east (SHIS) buried towards the south of the frame by ice flow from the east/north-east (IHIS). [Color figure can be viewed at [wileyonlinelibrary.com](http://wileyonlinelibrary.com)]

troughs. Individual ridges vary in width from 100 m to 8 km, and in orientation from north–south to east–west. Larger-scale features are predominately located to the west of the Malin Deep and orientated north–south, while smaller-scale features are observed to the south of the Malin Deep, with a more east–west trend.

A broad BPI analysis (radius of 5000 m) reveals a set of NNW–NW–orientated curvilinear ridges extending from west of the Malin Deep to the shelf edge (Figs 7a and 8b,f). Two of these ridges have been previously described by Dunlop *et al.* (2010) and included in recent glacial landform databases (Clark *et al.*, 2018). Our results identify at least one further ridge to the west and two to the east of similar scale and orientation to the features previously identified (Figs 7c and 8a). At this scale of analysis, the ridge sets are more difficult to recognize to the south, being gradually overprinted by smaller-scale landforms (see below). The 5000 m BPI analysis also highlights narrower, NW–SE–orientated arcuate ridges to the SW of the Malin Deep (Figs 7a and 8c) described by Dunlop *et al.* (2010) and also included in Clark *et al.* (2018). South-east of these narrower ridges, we identify a broad bathymetric high (seen in profile on Fig. 5) that slopes gently to the south-west across a drop of 13 m over 8 km (Fig. 8d).

A finer BPI analysis using a 1000 m radius reveals smaller-scale ridges on the southern flank of the Malin Deep (Figs 7b and 8e). The closely spaced ridges are 0.1–2 km wide, 0.5–4 m high and can be traced for up to 40 km. SB profiles indicate that they are formed in outcrops of S5 and S2 (Fig. 4d). Two sets of ridges are observed which differ in distribution and orientation. The northerly suite (Fig. 8e,f) is south of the Malin Deep and trends ENE/WSW. The second suite is north-west of Malin Head and generally trends east–west. The two sets converge south of the Malin Deep (Fig. 8e) and terminate at the larger NW-trending ridges occupying the broad bathymetric platform described above (Figs 7b and 8c,d). Dunlop *et al.* (2010) interpreted these small-scale ridges as post-glacial sand ribbons based on surface morphology, seabed type and orientation relative to dominant water currents. However, our interpretation of SB profiles shows them to be formed from the moulding of sediments comprising both S5 and S2 at the seabed, indicating a glacial origin.

#### *Interpretation of buried and seafloor landforms*

The seafloor and subsurface horizon landforms described above we interpret as cross-sections through glacial features corresponding in three dimensions to subglacial erosional

valleys, moraine ridges, streamlined ridges and GZWs (Fig. 8). These features are mainly associated with the erosional episodes that formed R2 and moulding of the overlying sediments comprising S5. We interpret them to have formed under sub-glacial to ice-proximal conditions during the Late Devensian cycle of ice sheet advance and subsequent retreat from the shelf edge.

Broad east–west subsurface depressions into S2 and S4 (the Malin and Stanton Formations, respectively) along R2 are interpreted to have formed via selective linear glacial erosion by topographically controlled ice flows across the Malin Shelf during the LGM. These valleys within the Malin Deep derive from erosion by ice flows from Scottish sources (Fig. 4). The R2 unconformity delineates two smaller valleys within the overall Malin Deep, termed here for the first time (Fig. 6). The larger Malin Deep Trough can be traced laterally northwards and is associated with erosion by ice of a Scottish ice source located to the north of the Stanton Banks. The smaller Isle of Mull Trough is orientated to the north-east towards Mull. Ice flows associated with the erosion of these valleys would have converged in the Malin Deep, where a buried ridge is observed (labelled in Fig. 4d, which can be traced in adjacent SB profiles; Supporting Information, Fig. S2). Based on its lateral extension, dimensions and location, we interpret the ridge as a buried medial shear moraine, indicative of the junction zone between two ice flows, possibly travelling at different velocities (Batchelor and Dowdeswell, 2016). To the south of this ridge the undulating R2 surface at the base of S5 (Fig. 4d) is interpreted as having been caused by the ploughing of S2 by ice keel penetration from the east by an overlying ice stream (cf. Clark *et al.*, 2003; Rippin *et al.*, 2014), processes identified in association with other marine-based palaeo-ice streams (Ó Cofaigh *et al.*, 2005). Clark *et al.* (2003) predict groove ploughing at the ice-stream base to occur downstream of regions where basal-roughness elements are produced. Here, upstream exposed bedrock in the Inner Hebrides Trough, or flow convergence producing subvertical shear planes within the ice stream, may have yielded an uneven ice base.

The incision of R2 into S2 north of the Donegal coastline (Fig. 5) is interpreted as an erosional feature formed by onshore to offshore ice flow from north County Donegal. The channel feature extends north-westwards up to 50 km from the Donegal coast (Supporting Information, Fig. S3) and is down ice of the submerged streamlined bedrock at the seabed near Tory Island (Benetti *et al.*, 2010). The regularly undulating top surface of the channel infill (S5b) is morphologically similar and within the scale boundaries of mega-scale glacial lineations (MSGs) observed at the seabed on recently glaciated continental margins (Ó Cofaigh *et al.*, 2005; Bellwald *et al.*, 2018). MSGs can occur downstream of streamlined bedrock (Clark *et al.*, 2003), in sequences of overlying multiple tills with inferred differences in consolidation (Dowdeswell *et al.*, 2004; Ó Cofaigh *et al.*, 2005), with ridges/grooves clustered closer together in areas of thicker sediment (Stokes, 2018), all observed here. These undulations on R2 are therefore interpreted to represent the streamlining of the subglacial bed into MSGs by fast-moving phase(s) of localized ice flow emanating from the north-west sector of the Irish Ice Sheet, and subsequently buried.

On the seafloor west of the Malin Deep, and in line with previous studies of the area (Dunlop *et al.*, 2010; Callard *et al.*, 2018), we interpret the broad ridges in S5 as GZWs. This interpretation is consistent with their truncated top surfaces, low height to length ratios and north–south orientation, orthogonal to reconstructed Scottish ice flow directions (Batchelor and Dowdeswell, 2015). Two of these ridges have been previously inferred to represent GZWs and are the largest

found on the Malin Shelf (Clark *et al.*, 2018). BPI analysis (Fig. 7a) identifies three further GZWs which are partially obscured by superimposed drumlins and iceberg furrows at the seabed (Fig. 8b). At the southern limit of these GZWs there is evidence of overprinting by MSGs (Fig. 8f), and previously reported drumlinoids and iceberg scours (Dunlop *et al.*, 2010).

South-west of the Malin Deep, we interpret the narrow moraines (Fig. 8c) described by Dunlop *et al.* (2010) and dated by Callard *et al.* (2018) to also represent GZWs. These ridges differ in orientation to those described above, which they appear to overprint. They also lack the overprinting by younger glacial landforms of the more northern GZWs. We interpret these GZWs as also originating from Scottish ice, with reduced extents possibly indicating lower sediment supply rates and/or occupation time of the ice sheet margin at these locations. As these GZWs overprint those to the north, and are not themselves overprinted, we attribute them to a later phase (second generation) of GZW formation. Up-ice on the southern margins of the Malin Deep we interpret ENE–WSW-trending curvilinear ridges at the seabed orientated in the direction of the GZWs as sets of coeval MSGs cut in S5 and S2 (Fig. 8c,e).

South of the Malin Deep, E–W-trending elongate ridges in S5 and S2 are also inferred to be MSGs formed by ice flow from the direction of the North Channel (Fig. 8d,e). These ridges lie adjacent to drumlins and iceberg scour lines but have not been overprinted by drumlins nor scoured themselves. To the east, the ridges terminate at a N–S-orientated low-amplitude broad ridge (GZW on Fig. 8d) also interpreted to represent a GZW, with more northern MSGs deflecting to the south-west around this ridge.

On the eastern margin of the Malin Deep, stacked asymmetrical mounds within S5 (Fig. 4) are interpreted as buried GZWs or sub-marginal till wedges (Dowdeswell and Fugelli, 2012; Batchelor and Dowdeswell, 2015) formed by ice originating from the Inner Hebrides Trough. Inferred ice-marginal positions occupy higher elevation locations inland and east of the Malin Deep, and given its stratigraphic position the constructional topography is interpreted as third-generation depositional features post-dating ridges nearer the shelf edge. Similarly to the north on the inner shelf in the Stanton Trough Callard *et al.* (2018) identified GZWs back stepping to the south-east during latter stages shelf deglaciation (23.2 ka BP). The observed stacking of S5 wedges (Fig. 4) indicates occupation of the shelf east of the Malin Deep by an oscillating grounded glacial margin contemporaneously with infilling of the Malin Deep by the glaciomarine sediments of S6 (Jura Formation).

## Discussion

### *Multiple ice streams on the Malin Shelf*

Consistent with previous studies of the Malin Shelf, the sediment record presented above provides evidence of at least two cycles of glacial occupation, the younger dated to the LGM. We show this younger cycle to contain an assemblage of subsurface and seafloor glacial landforms recording ice flow patterns across the shelf and deposition during ice margin retreat. We interpret the LGM landform assemblage to record multiple independent ice streams that extended to the outer Malin Shelf (Fig. 9).

Multiple ice streams have previously been inferred for the region (Dunlop *et al.*, 2010; Ó Cofaigh *et al.*, 2012; Dove *et al.*, 2015; Clark *et al.*, 2018), converging on the Malin Shelf to form what has been referred to as the HIS (Howe *et al.*, 2012;

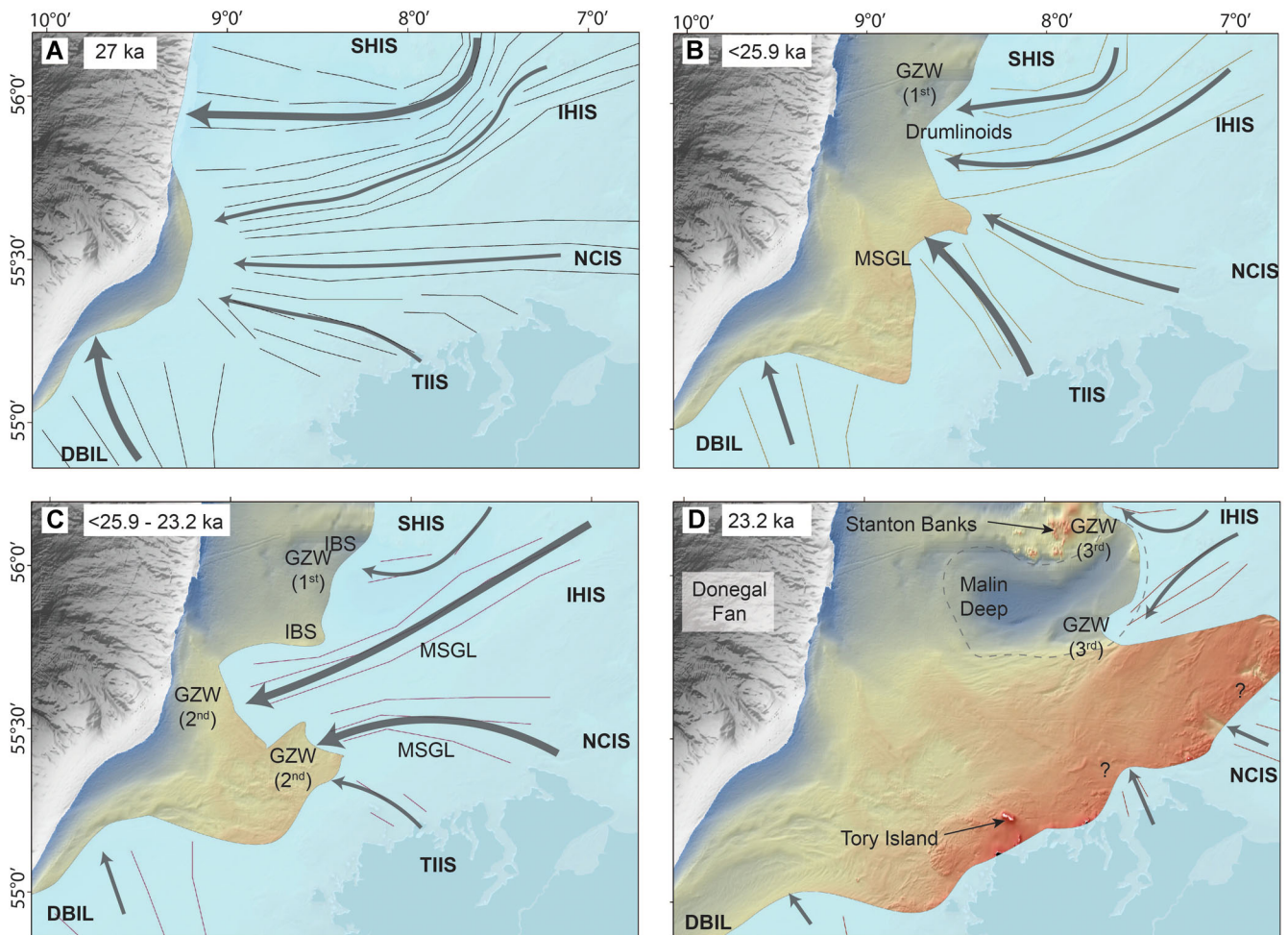


**Figure 9.** Hypothesized reconstruction of LGM ice history on the Malin Shelf. The age model is based on dating reported by Callard *et al.* (2018). Arrows indicate the reconstructed flow paths of different ice streams. Solid and dashed lines indicate glacial geomorphologies described in the text at their inferred time of formation. GZW = grounding zone wedge (1st to 3rd generation – see text), MSGL = mega-scale glacial lineation, IBS = iceberg scours. (A) Local LGM ice extent to the shelf edge with dominant Sea of the Hebrides Ice Stream (SHIS) and Donegal Bay Ice Lobe (DBIL) (Ó Cofaigh *et al.*, 2019) constraining the seaward flow of TIIS and NCIS. (B) SHIS grounding line retreat in response to glacial dynamics north of Stanton Banks (Fig. 1) permits a northward Tory Island Ice Stream (TIIS) advance onto the shelf with possible northward deflection of the North Channel Ice Stream (NCIS) and Inner Hebrides Ice Stream (IHIS). (C) Further retreat of SHIS grounding line along reverse bed slopes causes reorganization of ice sheet with the IHIS and NCIS advancing across the shelf. (D) Rapid retreat of all areas of the ice margin to stable pinning points; GZWs form along the IHIS marine margin, while a marine embayment forms north-west of Donegal. [Color figure can be viewed at [wileyonlinelibrary.com](http://wileyonlinelibrary.com)]

Dove *et al.*, 2016; Callard *et al.*, 2018). However, our results provide direct evidence of four main component ice streams that extended to the mid- to outer shelf from both Scottish and Irish sources. We name these component ice streams the Sea of the Hebrides Ice Stream (SHIS), the Inner Hebrides Ice Stream (IHIS), the North Channel Ice Stream (NCIS) and the Tory Island Ice Stream (TIIS), and show them to provide new information on the pattern of shelf deglaciation following the LGM.

The SHIS is proposed to originate north of the study area. Its flow path was strongly topographically controlled, occupying the Sea of the Hebrides Trough and deflecting around the Stanton Banks before entering the study region along the line of the Stanton Trough. The evidence for this includes the over-deepened buried Malin Deep Trough closing towards the Stanton Trough (Fig. 6b), the large first-generation N–S-orientated GZWs to the west of the Malin Deep (Fig. 8b) and the buried shear moraine (Fig. 4d) representing the southern limit of its influence. We interpret this ice stream as an extension of the Hebridean Ice Stream originating from the Outer Hebrides (Howe *et al.*, 2012).

The IHIS is proposed to originate north-east of the study area, occupying the Inner Hebrides Trough and converging with the SHIS south of the Stanton Trough. The evidence for

this includes the buried Isle of Mull Trough which closes towards the Inner Hebrides Trough (Fig. 6b); buried ice keel ploughing (Fig. 4d); second-generation NW–SE-orientated GZWs to the south-west of the Malin Deep (Fig. 7c); the WSW-orientated MSGLs on the southern flank of the Malin Deep (Fig. 8e) which deflect around the southern GZW/marginal till wedge (Fig. 8c); and iceberg scours on the western margin of the Malin Deep (Fig. 8f). The MSGLs and iceberg scours overprint the first-generation GZWs of the SHIS. We interpret the IHIS as an extension of the ice stream previously described by Dove *et al.* (2016) from the Inner Hebrides.

The NCIS is proposed to originate to the east of the study area, flowing over the bathymetric platform south of the Malin Deep. The evidence for this comprises the E–W-orientated MSGL terminating at the most southern second-generation GZW/marginal till wedge (Fig. 7c). We interpret the NCIS as an extension of ice originating from the North Channel Ice Divide of Finlayson *et al.* (2014).

Finally, the TIIS is proposed to flow offshore from central north County Donegal. The evidence comprises a buried channel, buried MSGLs and back-stepping sedimentary packages (Fig. 5). We interpret this ice stream to be the ice flow also responsible for the formation of the drumlin field at seabed near Tory Island (Benetti *et al.*, 2010; Supporting Information, Fig. S3).

We thus infer that at least four ice streams were coeval and coincident on the Malin Shelf during the last deglaciation and that they interacted and varied in size and strength. We propose that the SHIS originating from north of the Stanton Banks was the largest and most dominant ice stream in the area. The SHIS coalesced with the IHIS south of the Stanton Banks. Mapping of flow patterns indicates that the smaller IHIS was deflected southwards by the SHIS seaward of the topographic barrier of Coll and Tíree (Fig. 9a), forming the Isle of Mull Trough.

Both these northern ice streams are likely to have been larger than either the NCIS or the TIIS, which did not create over-deepened troughs and are inferred to have been restricted in extension to close to the north Irish coastline (Fig. 9a) with the exception of some late-stage possibly rapid and short-lived expansions recorded by streamlined landform sets both buried and at the seabed. The dominance of combined Scottish ice input over ice from less extensive Irish sources supports traditional models of ice sheet geometry and distinguishes our reconstruction from models that envisage a more balanced convergence of equivalent ice streams (Bradwell *et al.*, 2008; Scourse *et al.*, 2009; Dunlop *et al.*, 2010).

### *Hypothesized interaction and deglacial retreat of ice streams*

Our interpretation of the Malin Shelf sedimentary record is consistent with models of an episodic multi-stage ice retreat pattern from shelf-edge LGM extents which has been observed in other post-LGM glaciated marine-terminating margins, where ice buttressing is reduced (Winsborrow *et al.*, 2010; Sejrup *et al.*, 2016). We propose that in the southern sector of the Malin Shelf, the HIS comprised a dynamic ice stream complex that underwent phased, episodic but rapid retreat from the shelf edge.

Initial deglaciation from the Malin Shelf edge, north of the Stanton Banks, along the margin of the HIS by 26.7 ka BP (Callard *et al.*, 2018) occurred during global sea-level lower stands (Lambeck *et al.*, 2014) and local sea-surface temperature cooling (Peck *et al.*, 2008; Hibbert *et al.*, 2010). Deglaciation therefore cannot be readily explained by either global sea-level rise or temperature increases. Callard *et al.* (2018) proposed localized relative sea-level rise due to isostatic loading by the BIIS as a mechanism to create tidewater ice-marginal conditions across the shelf, causing destabilization and rapid deglaciation of the Malin Deep along reverse bed slopes.

However, our evidence of overprinted glacial landform assemblages indicates a more nuanced dynamic of deglaciation, involving interactions between four converging ice streams on the Malin Shelf. We propose that at the LGM the SHIS was the dominant regional ice stream on the Malin Shelf and acted as a buttress constraining the smaller southern ice streams of the IHIS, NCIS and TIIS, leading to constraint in flow out of their source areas. This conforms with other recorded observations of a dominance of SHIS ice flow (Small *et al.*, 2017) with little westward flow in southern parts of the shelf (Finlayson *et al.*, 2014).

At and immediately following the LGM in the region (~26–27 ka), multiple GZWs on the western margin of the Malin Deep support models of staged retreat of the SHIS from shelf edge positions (Ó Cofaigh *et al.*, 2008; Callard *et al.*, 2018), although these landforms are yet to be directly dated. We suggest that rapid deglaciation of the SHIS along the axis of the Malin Deep mirrored that of the HIS north of the Stanton Banks (Callard *et al.*, 2018) and was initiated by unpinning of the SHIS from the more elevated reverse slope region on the outer shelf before 26.7 ka (Fig. 9). Rapid deglaciation was facilitated by eastward

deepening of ice-marginal water depths within the Malin Deep. Given the probable connectivity of the SHIS to other northern HIS sectors in the Sea of the Hebrides, the SHIS may have been dynamically responsive to the drawdown of ice seaward along these northern sectors, and thus acted almost independently of other ice streams on the Malin Shelf, south of the Stanton Banks. Despite wide coverage by seismic reflection profiles, we find no evidence of buried GZWs within the Malin Deep, which we argue to be consistent with a rapid retreat of the SHIS to stable pinning points on the inner-shelf following shelf edge deglaciation from 26 to ~20 ka (Small *et al.*, 2017; Callard *et al.*, 2018).

IRD analysis from a core taken from the Barra Fan (Knutz *et al.*, 2001), linked to sediment supply along the HIS north of the Stanton Banks, shows millennial-scale fluctuations in Scottish-sourced IRD commencing at 30 ka and continuing to about 22 ka, demonstrating a dynamic and fluctuating ice margin north of the study area. An IRD peak in the core is dated to just <28.6 ka BP, earlier than the initial deglaciation dates of Callard *et al.* (2018) with another larger, undated one, following shortly after (Knutz *et al.*, 2001). While IRD peaks cannot be linked definitively to ice margin behaviour, ice marginal retreat is a key mechanism that increases IRD supply. These IRD peaks therefore could indicate initial destabilization of the SHIS located nearby, south of the Stanton Banks. We propose that the SHIS also supplied sediment to the Malin Shelf edge to the south of the Barra Fan, and may account for sediment aggradation on the Donegal Fan lobe of the Donegal–Barra Fan complex.

We propose that retreat of the SHIS began early in terms of the LGM timing, and before other ice discharges onto the Malin Shelf. This rapid retreat of a dominant ice stream probably impacted the dynamics of converging ice streams to the south, similar to the impacts of buttressing and unconstraining observed and modelled elsewhere (Winsborrow *et al.*, 2010; Sejrup *et al.*, 2016; Gandy *et al.*, 2018). In particular, this may have released cross-shelf flow constraints on the other Malin Shelf ice streams leading to opportunities for rapid ice-marginal advances along several fronts during the overall LGM. Our mapping of seismic unit distributions to the south of the Malin Deep show that sediments streamlined by the TIIS underlie packages associated with the IHIS and NCIS. This indicates a relatively early extension of the TIIS across the shelf, possibly because of its source area proximity and the persistence of strong localised ice dispersal centres in NW Ireland over the duration of the LGM (McCarron, 2013). Wilson *et al.* (2019) reconstruct LGM ice supply to a 'Malin Shelf Ice Stream' from northern Donegal and with its decoupling resulting in the presence of a marine embayment along the north Donegal coast by 22–21 ka. Relatively early advance of north Donegal ice onto the shelf supports our proposed relative chronology and propose that dynamic processes facilitated accelerated discharge of ice and ice streaming along the TIIS before 22 ka.

As indicated by the morphosedimentary stratigraphy on the shelf region north of the Irish coastline and south of the Malin Deep, following retreat of the TIIS, the IHIS and NCIS extended rapidly in a single advance across the Malin Shelf (Fig. 9c). Less extensive GZWs marking maximum ice extents of the IHIS and NCIS indicate that these ice streams had small ice volumes and/or sediment supply compared to the SHIS. Landforms and sediment units associated with the IHIS and NCIS overlie those associated with the TIIS as well as the GZWs of the SHIS, forming the drumlin swarm observed by Dunlop *et al.* (2010). The second-generation GZWs developed by these ice streams are better preserved than the earlier GZWs of the SHIS with no subsequent reworking by glacial processes. The rapid extension of both ice streams across the pre-existing sediment cover is indicated by the formation of extensive MSGL suites now at the seabed. These trend NE–SW from the Inner Hebrides

Trough, and east–west from the direction of the North Channel/SW Scotland. Both sets terminate at the proposed down-ice margin of the second-generation GZWs associated with the reconstructed ice streams. IHIS and NCIS streaming is proposed to have been contemporaneous as the MSGL suites of both streams converge. The MSGLs linked to the IHIS are subsequently deflected down ice around the terminal sediment wedge associated with the NCIS (Fig. 8c). The more westward GZW is associated with the IHIS and possibly indicates it was the larger of the two. Small *et al.* (2017) tentatively date these GZWs to 24 ka based on a palaeoglaciological model of ice sheet reorganization processes associated with Heinrich Event 2 and IRD delivery peak to the Barra Fan at that time (Scourse *et al.*, 2009). Callard *et al.* (2018) date this extension to between  $26.7 \pm 0.3$  and  $25.3 \pm 0.3$  ka BP.

Several lines of evidence point to rapid retreat of the TIIS, IHIS and NCIS following extension across the shelf: (i) the presence and preservation of MSGLs at the seafloor related to the IHIS and NCIS; (ii) the preservation of buried glacial geomorphology associated with the TIIS and IHIS; and (iii) the absence of recessional moraines or GZWs across the mid shelf. Stacked GZWs (in S5) interfingering with known glaciomarine sediments at the mouth of the Inner Hebrides Trough on the landward side of the Isle of Mull Trough are consistent with an oscillating marine-terminating margin at this location. A radiocarbon date indicates that ice margins occupied this location  $<23.2 \pm 0.3$  ka BP (Callard *et al.*, 2018). The alternating open water and sub-ice marginal deposition sequence at the mouth of the Inner Hebrides Trough supports the interpretation of tidewater margin retreat within this trough. This has been inferred to explain the deposition of buried GZWs further landward (Arosio *et al.*, 2018) and suggests the GZWs in the Stanton Trough (Callard *et al.*, 2018) also formed during deglaciation of the IHIS. There is no evidence of later ice advance with terrestrial cosmogenic nuclide dating limiting deglaciation of Tiree (Fig. 2) to  $20.6 \pm 1.2$  ka (Small *et al.*, 2017) and the formation of ice-distal environments in the inner shelf by  $16.8 \pm 0.2$  ka (Callard *et al.*, 2018).

## Conclusions

We use legacy geophysical datasets, comprising multibeam bathymetric data and seismic profiles of varying frequency content to present an interpretation of seafloor and buried glacial landforms on the Malin Shelf south of the Stanton Banks. The results allow a new reconstruction of the patterns of ice margin retreat from the shelf edge at the LGM (27–22 ka). Based on the orientation and distribution of GZWs, MSGLs, ice keel ploughing and shear moraines (primarily within S5 – Barra Formation) we propose that the time-transgressive retreat of the ice sheet margin across the shelf involved at least four independent ice streams of varying strength. Rather than a single ‘Hebrides Ice Stream’ on the Malin Shelf as previously envisaged, we argue for a more nuanced picture of ice stream generation, chronology and control that considers ice stream interaction, buttressing and unconstraining are required to understand the resulting landform assemblages. We propose the larger northern SHIS occupied the Malin Shelf and buttressed southern ice streams. In response to the rapid retreat of SHIS from the shelf edge along the Malin Deep following the local LGM, the three southern ice streams (TIIS, IHIS and NCIS) experienced post-LGM phased rapid extension and retreat as a direct result of unconstraining. The operation of multiple separate ice streams on the Malin Shelf proposed here fits well with: (i) models of ice streaming observed in Donegal, landform sequences and deglacial events in the Inner Hebrides; and (ii) the occurrence of drumlin swarms on the Malin Shelf and

changes in the flow direction of North Channel Ice. Our findings highlight the importance of understanding the interactions of converging ice streams, with implications for modern marine-terminating ice margins.

## Supporting information

Additional supporting information may be found in the online version of this article at the publisher’s web-site.

**Figure S1.** Extent of 176 INSS 2003 sub-bottom lines interpreted for this study. This is a subset of all INSS crosslines and approximately 20% of surveyed mainlines across the shelf.

**Figure S2.** Selected sub-bottom profiles: (A) line positions N–S across the Malin Deep; (B) interpretation. Separate channels infilled with S6 merge down ice between sub-bottom lines 0422 and 0413. Highly undulated R2 and top S5 (with triangles) persist beneath the southern channel (IHIS). Ridge topography exists at the boundary between two channels, developing into the interpreted shear moraine referred to in the text. Infilled by S6 with representative bed geometry included.

**Figure S3.** Mapped northern distribution of TIIS-deposited sediment extent (Fig. 5b,d) from 2003 INSS crosslines. Sedimentary package remains confined within an ~16-km-wide channel-like feature, which does not extend north of the buried bathymetric high formed by S2 (Fig. 5d) and would have provided a stable pinning point. Hypothesized extent of TIIS illustrated.

*Acknowledgements.* Funding for this work was provided through an Irish Research Council Enterprise Partnership Scheme postdoctoral award EPSD/2015/19. The authors wish to thank the Department of the Environment, Climate and Communications for free dissemination of geophysical data from the INSS programme and the Petroleum Affairs Division. MESH sparker profiles are from British Geological Survey materials and obtained under licence (© NERC). We greatly appreciate the thoughtful and constructive feedback of two anonymous reviewers that greatly improved the focus and clarity of the manuscript. Final thanks are given to Marine Institute staff, Masters and crews of the Celtic Voyager for their invaluable assistance and persistence over the duration of the research project and the wider INSS/INFOMAR programmes.

## Data availability statement

INSS bathymetry and sub-bottom datasets related to this article can be found at <https://www.infomar.ie/data> available through the Interactive Web Data Delivery System or by contacting [info@infomar.ie](mailto:info@infomar.ie). MESH sparker profiles can be found at [https://mapapps2.bgs.ac.uk/geoindex\\_offshore/home.html](https://mapapps2.bgs.ac.uk/geoindex_offshore/home.html) available through the National Geoscience Data Centre. Metadata related to multi-channel seismic profiles and offshore well data can be accessed via <https://data.gov.ie/dataset> with data available under licence by contacting [dataep.info@decc.gov.ie](mailto:dataep.info@decc.gov.ie). All other data are available from the corresponding author.

*Abbreviations.* BIIS, British–Irish Ice Sheet; BPI, bathymetric positioning index; DEM, Digital Elevation Model; GZW, grounding zone wedge; IHIS, Inner Hebrides Ice Stream; INSS, Irish National Seabed Survey; LAT, lowest astronomical tide; MCS, multichannel seismic; MESH, Mapping European Seabed Habitats; MSGL, mega-scale glacial lineation; NCIS, North Channel Ice Stream; SB, sub-bottom; SHIS, Sea of the Hebrides Ice Stream; TIIS, Tory Island Ice Stream.

## References

Armishaw JE, Holmes RW, Stow DA. 1998. Morphology and sedimentation on the Hebrides Slope and Barra Fan, NW UK continental margin. In *Geological Processes on Continental*

- Margins: Sedimentation, Mass-wasting and Stability*, Stoker MS, Evans D, Cramp A (eds). Special Publications. **129** London: Geological Society, 81–104.
- Armishaw JE, Holmes RW, Stow DAV. 2000. The Barra Fan: a bottom-current reworked, glacially fed submarine fan system. *Marine and Petroleum Geology* **17**: 219–238.
- Arosio R, Dove D, Ó Cofaigh C *et al.* 2018. Submarine deglacial sediment and geomorphological record of southwestern Scotland after the Last Glacial Maximum. *Marine Geology* **403**: 62–79.
- Bamber JL, Vaughan DG, Joughin I. 2000. Widespread complex flow in the interior of the Antarctic ice sheet. *Science* **287**: 1248–1250.
- Batchelor CL, Dowdeswell JA. 2015. Ice-sheet grounding-zone wedges (GZWs) on high-latitude continental margins. *Marine Geology* **363**: 65–92.
- Batchelor CL, Dowdeswell JA. 2016. Lateral shear-moraines and lateral marginal-moraines of palaeo-ice streams. *Quaternary Science Reviews* **151**: 1–26.
- Bellwald B, Planke S, Piasecka ED *et al.* 2018. Ice-stream dynamics of the SW Barents Sea revealed by high-resolution 3D seismic imaging of glacial deposits in the Hoop area. *Marine Geology* **402**: 165–183.
- Benetti S, Dunlop P, Cofaigh C. 2010. Glacial and glacially related features on the continental margin of northwest Ireland mapped from marine geophysical data. *Journal of Maps* **6**: 14–29.
- Binns PE, Harland R, Hughes MJ. 1974. Glacial and postglacial sedimentation in the Sea of the Hebrides. *Nature* **248**: 751–754.
- Bowen DQ, Phillips FM, McCabe AM *et al.* 2002. New data for the last glacial maximum in Great Britain and Ireland. *Quaternary Science Reviews* **21**: 89–101.
- Bradwell T, Stoker M. 2014. Asymmetric ice-sheet retreat pattern around northern Scotland revealed by marine geophysical surveys. *Earth and Environmental Science Transactions of the Royal Society of Edinburgh* **105**: 297–322.
- Bradwell T, Stoker MS, Golledge NR *et al.* 2008. The northern sector of the last British Ice Sheet: maximum extent and demise. *Earth-Science Reviews* **88**: 207–226.
- Brown EJ, Rose J, Coope RG *et al.* 2007. An MIS 3 age organic deposit from Balglass Burn, central Scotland: palaeoenvironmental significance and implications for the timing of the onset of the LGM ice sheet in the vicinity of the British Isles. *Journal of Quaternary Science* **22**: 295–308.
- Callard SL, Cofaigh C, Benetti S *et al.* 2018. Extent and retreat history of the Barra Fan Ice Stream offshore western Scotland and Northern Ireland during the last glaciation. *Quaternary Science Reviews* **201**: 280–302.
- Clark CD, Ely JC, Greenwood SL *et al.* 2018. BRITICE Glacial Map, version 2: a map and GIS database of glacial landforms of the last British-Irish Ice Sheet. *Boreas* **47**: 11–e8.
- Clark CD, Hughes ALC, Greenwood SL *et al.* 2012. Pattern and timing of retreat of the last British-Irish Ice Sheet. *Quaternary Science Reviews* **44**: 112–146.
- Clark CD, Tulaczyk SM, Stokes CR *et al.* 2003. A groove-ploughing theory for the production of mega-scale glacial lineations, and implications for ice-stream mechanics. *Journal of Glaciology* **49**: 240–256.
- Craig D, Welding P. 2006. *End of Well Report: 13/12-1 Inishbeg Prospect (Well Report)*. Lundin Exploration B.V.
- Cross TA, Lessenger MA. 1988. Seismic stratigraphy. *Annual Review of Earth and Planetary Sciences* **16**: 319–354.
- Cullen S. 2003. Irish National Seabed Survey – an introductory overview. *Hydrographic Journal* **109**: 22–25.
- Davies HC, Dobson MR, Whittington RJ. 1984. A revised seismic stratigraphy for Quaternary deposits on the inner continental shelf west of Scotland between 55°30'N and 57°30'N. *Boreas* **13**: 49–66.
- Dove D, Arosio R, Finlayson A *et al.* 2015. Submarine glacial landforms record Late Pleistocene ice-sheet dynamics, Inner Hebrides, Scotland. *Quaternary Science Reviews* **123**: 76–90.
- Dove D, Finlayson A, Bradwell T *et al.* 2016. Deglacial landform assemblage records fast ice-flow and retreat, Inner Hebrides, Scotland. *Geological Society, London, Memoirs* **46**: 135–138.
- Dowdeswell JA, Cofaigh C, Pudsey CJ. 2004. Thickness and extent of the subglacial till layer beneath an Antarctic paleo-ice stream. *Geology* **32**: 13–16.
- Dowdeswell JA, Fugelli EMG. 2012. The seismic architecture and geometry of grounding-zone wedges formed at the marine margins of past ice sheets. *Geological Society of America Bulletin* **124**: 1750–1761.
- Dowdeswell JA, Ottesen D, Evans J *et al.* 2008. Submarine glacial landforms and rates of ice-stream collapse. *Geology* **36**: 819–822.
- Dunlop P, Shannon R, McCabe M *et al.* 2010. Marine geophysical evidence for ice sheet extension and recession on the Malin Shelf: new evidence for the western limits of the British Irish Ice Sheet. *Marine Geology* **276**: 86–99.
- Evans D, Kenolty N, Dobson MR *et al.* 1980. The geology of the Malin Sea. <http://pubs.bgs.ac.uk/publications.html?pubID=B01156>
- Eyles N, McCabe AM. 1989. The Late Devensian (<22,000 BP) Irish Sea Basin: the sedimentary record of a collapsed ice sheet margin. *Quaternary Science Reviews* **8**: 307–351.
- Finlayson A, Fabel D, Bradwell T *et al.* 2014. Growth and decay of a marine terminating sector of the last British-Irish Ice Sheet: a geomorphological reconstruction. *Quaternary Science Reviews* **83**: 28–45.
- Fyfe JA, Long D, Evans D. 1993. *The Geology of the Malin-Hebrides Sea Area*. British Geological Survey, United Kingdom Offshore Regional Report. HMSO: London.
- Gandy N, Gregoire LJ, Ely JC *et al.* 2018. Marine ice sheet instability and ice shelf buttressing of the Minch Ice Stream, northwest Scotland. *The Cryosphere* **12**: 3635–3651.
- Greenwood SL, Clark CD. 2009a. Reconstructing the last Irish Ice Sheet 2: a geomorphologically-driven model of ice sheet growth, retreat and dynamics. *Quaternary Science Reviews* **28**: 3101–3123.
- Greenwood SL, Clark CD. 2009b. Reconstructing the last Irish Ice Sheet 1: changing flow geometries and ice flow dynamics deciphered from the glacial landform record. *Quaternary Science Reviews* **28**: 3085–3100.
- Hibbert FD, Austin WEN, Leng MJ *et al.* 2010. British Ice Sheet dynamics inferred from North Atlantic ice-rafted debris records spanning the last 175 000 years. *Journal of Quaternary Science* **25**: 461–482.
- Howe JA, Anderton R, Arosio R *et al.* 2014. The seabed geomorphology and geological structure of the Firth of Lorn, western Scotland, UK, as revealed by multibeam echo-sounder survey. *Earth and Environmental Science Transactions of the Royal Society of Edinburgh* **105**: 273–284.
- Howe JA, Dove D, Bradwell T *et al.* 2012. Submarine geomorphology and glacial history of the Sea of the Hebrides, UK. *Marine Geology* **315–318**: 64–76.
- Hubbard A, Bradwell T, Golledge N *et al.* 2009. Dynamic cycles, ice streams and their impact on the extent, chronology and deglaciation of the British-Irish ice sheet. *Quaternary Science Reviews* **28**: 758–776.
- King EL, Halfidason H, Sejrup HP *et al.* 1998. End moraines on the northwest Irish continental shelf. Presented at the 3rd ENAM II Workshop.
- Knutz PC, Austin WEN, Jones EJW. 2001. Millennial-scale depositional cycles related to British Ice Sheet variability and North Atlantic paleocirculation since 45 kyr B.P., Barra Fan, U.K. margin. *Paleoceanography* **16**: 53–64.
- Kokalj Ž, Zakšek K, Oštir K. 2011. Application of sky-view factor for the visualisation of historic landscape features in lidar-derived relief models. *Antiquity* **85**: 263–273.
- Lambeck K, Rouby H, Purcell A *et al.* 2014. Sea level and global ice volumes from the Last Glacial Maximum to the Holocene. *Proceedings of the National Academy of Sciences of the United States of America* **111**: 15296–15303.
- McCarron S. 2013. Deglaciation of the Dungiven Basin, north-west Ireland. *Irish Journal of Earth Sciences* **31**: 43–71.
- McCarron S, Praeg D, Ó Cofaigh C *et al.* 2018. A Plio-Pleistocene sediment wedge on the continental shelf west of central Ireland: the Connemara Fan. *Marine Geology* **399**: 97–114.
- Ó Cofaigh C, Dowdeswell JA, Allen CS *et al.* 2005. Flow dynamics and till genesis associated with a marine-based Antarctic palaeo-ice stream. *Quaternary Science Reviews* **24**: 709–740.

- Ó Cofaigh C, Weillbach K, Lloyd JM *et al.* 2019. Early deglaciation of the British–Irish Ice Sheet on the Atlantic shelf northwest of Ireland driven by glacioisostatic depression and high relative sea level. *Quaternary Science Reviews* **208**: 76–96.
- Ó Cofaigh C, Dowdeswell JA, Evans J *et al.* 2008. Geological constraints on Antarctic palaeo-ice-stream retreat. *Earth Surface Processes and Landforms* **33**: 513–525.
- Ó Cofaigh C, Dunlop P, Benetti S. 2012. Marine geophysical evidence for Late Pleistocene ice sheet extent and recession off northwest Ireland. *Quaternary Science Reviews* **44**: 147–159.
- Patton H, Andreassen K, Bjarnadóttir LR *et al.* 2015. Geophysical constraints on the dynamics and retreat of the Barents Sea ice sheet as a paleobenchmark for models of marine ice sheet deglaciation. *Reviews of Geophysics* **53**: 1051–1098.
- Peck VL, Hall IR, Zahn R *et al.* 2008. Millennial-scale surface and subsurface paleothermometry from the northeast Atlantic, 55–8 ka BP: NE Atlantic paleothermometry. *Paleoceanography* **23**: PA3221.
- Pollard D, DeConto RM. 2009. Modelling West Antarctic ice sheet growth and collapse through the past five million years. *Nature* **458**: 329–332.
- Rippin DM, Bingham RG, Jordan TA *et al.* 2014. Basal roughness of the Institute and Möller Ice Streams, West Antarctica: process determination and landscape interpretation. *Geomorphology* **214**: 139–147.
- Sayag R, Tziperman E. 2011. Interaction and variability of ice streams under a triple-valued sliding law and non-Newtonian rheology. *Journal of Geophysical Research: Earth Surface* **116**: F01009.
- Scourse JD, Haapaniemi AI, Colmenero-Hidalgo E *et al.* 2009. Growth, dynamics and deglaciation of the last British–Irish ice sheet: the deep-sea ice-rafted detritus record. *Quaternary Science Reviews* **28**: 3066–3084.
- Sejrup HP, Clark CD, Hjelstuen BO. 2016. Rapid ice sheet retreat triggered by ice stream debuttressing: evidence from the North Sea. *Geology* **44**: 355–358.
- Small D, Benetti S, Dove D *et al.* 2017. Cosmogenic exposure age constraints on deglaciation and flow behaviour of a marine-based ice stream in western Scotland, 21–16 ka. *Quaternary Science Reviews* **167**: 30–46.
- Stoker MS. 1995. The influence of glacial sedimentation on slope-apron development on the continental margin off northwest Britain. In *The Tectonics, Sedimentation and Palaeoceanography of the North Atlantic Region*, Scrutton, RA, Stoker, MS, Shimmield, GB, Tudhope, AW (eds). Geological Society Special Publications. London: Geological Society, **90**: 159–177.
- Stokes CR. 2018. Geomorphology under ice streams: moving from form to process. *Earth Surface Processes and Landforms* **43**: 85–123.
- Stuart. 1979. *Republic of Ireland Continental Shelf Oil Well Records: Final Geological Well Report; 13/3-1 (Final Geological Well Report No. 13/3-1)*. Petroleum Affairs Division.
- Szpak M. 2012. *Chemical and Physical Dynamics of Marine Pockmarks with Insights into the Organic Carbon Cycling on the Malin Shelf and in Dunmanus Bay, Ireland*. Dublin City University.
- Szpak MT, Monteys X, O'Reilly S *et al.* 2012. Geophysical and geochemical survey of a large marine pockmark on the Malin Shelf, Ireland. *Geochemistry, Geophysics, Geosystems* **13**: Q01011.
- Torbjørn Dahlgren KI, Vorren TO, Stoker MS *et al.* 2005. Late Cenozoic prograding wedges on the NW European continental margin: their formation and relationship to tectonics and climate. *Marine and Petroleum Geology* **22**: 1089–1110.
- Wallis DG. 2006. *Rockall-North Channel MESH Geophysical Survey, RRS Charles Darwin Cruise CD174, BGS Project 05/05 Operations Report*. Marine, Coastal and Hydrocarbons Programme Internal Report No. IR/05/132. BGS: Nottingham.
- Wilson LJ, Austin WEN. 2002. Millennial and sub-millennial-scale variability in sediment colour from the Barra Fan, NW Scotland: implications for British ice sheet dynamics, *Geological Society, London, Special Publications*, 349–365.
- Wilson MFJ, O'Connell B, Brown C *et al.* 2007. Multiscale terrain analysis of multibeam bathymetry data for habitat mapping on the continental slope. *Marine Geodesy* **30**: 3–35.
- Wilson P, Ballantyne CK, Benetti S *et al.* 2019. Deglaciation chronology of the Donegal Ice Centre, north-west Ireland. *Journal of Quaternary Science* **34**: 16–28.
- Winsborrow MCM, Andreassen K, Corner GD *et al.* 2010. Deglaciation of a marine-based ice sheet: Late Weichselian palaeo-ice dynamics and retreat in the southern Barents Sea reconstructed from onshore and offshore glacial geomorphology. *Quaternary Science Reviews* **29**: 424–442.
- Zakšek K, Oštir K, Kokalj Ž. 2011. Sky-view factor as a relief visualization technique. *Remote Sensing* **3**: 398–415.
- Zhilin D, Sheridan D. 2003. *Irish National Seabed Survey, Survey Report Leg CE03\_02 Zone 2 (Cruise Report)*. Geological Survey of Ireland.